NASA CR-168036
R82AEB399

National Aeronautics and
Space Administration

ENERGY EFFICIENT ENGINE

HIGH PRESSURE TURBINE CERAMIC SHROUD SUPPORT TECHNOLOGY REPORT

November 1982

By

W.A. Nelson

R.G. Carlson

AIRCRAFT ENGINE BUSINESS GROUP
ADVANCED TECHNOLOGY PROGRAMS DEPARTMENT
CINCINNATI, OHIO 45215

Prepared for

NATIONAL AERONAUTICS AND SPACE ADMINISTRATION
LEWIS RESEARCH CENTER
21000 BROOKPARK ROAD
CLEVELAND, OHIO 44135

NASA - LEWIS RESEARCH CENTER
Contract NAS3-20643

1. Report No.	2. Government Accession No.	3. Recipient's Catalog No.
NASA CR-168036		

4. Title and Subtitle	5. Report Date
Energy Efficient Engine High Pressure Turbine Ceramic Shroud Support Technology Report	November 1982
	6. Performing Organization Code

7. Author(s)	8. Performing Organization Report No.
W.A. Nelson R.G. Carlson	R82AEB399
	10. Work Unit No.

9. Performing Organization Name and Address	11. Contract or Grant No.
General Electric Company Aircraft Engine Business Group Cincinnati, Ohio 45215	NAS3-20643
	13. Type of Report and Period Covered

12. Sponsoring Agency Name and Address	14. Sponsoring Agency Code
National Aeronautics and Space Administration Washington, D.C. 20546	

15. Supplementary Notes

NASA Project Manager - Mr. C.C. Ciepluch G.E. Project Manager - R.W. Bucy
NASA Project Engineer - Mr. T. Strom

16. Abstract

This work represents the development and fabrication of ceramic HPT (high pressure turbine) shrouds for the Energy Efficient Engine (E^3). Details are presented covering the work performed on the ceramic shroud development task of the NASA/GE Energy Efficient Engine (E^3) component development program. The task consists of four phases which led to the selection of a ZrO_2-$8Y_2O_3$ ceramic shroud material system, the development of an automated plasma spray process to produce acceptable shroud structures, the fabrication of select shround systems for evaluation in laboratory, component, and CF6-50 engine testing, and finally, the successful fabrication of ZrO_2-$8Y_2O_3$/superpeg, engine quality shrouds for the E^3 engine.

17. Key Words (Suggested by Author(s))	18. Distribution Statement
Plasma Spray Thermal Shock Ceramic Shroud Bond Coat	For Early Domestic Dissemination (PEDD)

19. Security Classif. (of this report)	20. Security Classif. (of this page)	21. No. of Pages	22. Price*

* For sale by the National Technical Information Service, Springfield, Virginia 22161

TABLE OF CONTENTS

LIST OF FIGURES AND TABLES

LIST OF FIGURES AND TABLES (Concluded)

TABLES

I. SUMMARY

This report describes the work performed on a multi-phased program to develop ceramic High Pressure Turbine (HPT) shrouds for the NASA/GE Energy Efficient Engine (E^3). The program consisted of four phases: 1) selection of a candidate shroud system, 2) development of that shroud system, 3) component testing, including CF6-50 engine testing, static laboratory testing, and development of quality control inspection method using non-descructive techniques, and 4) fabrication of hardware for E^3 engine testing. Examples of successfully tested ceramic shrouds are shown in Figure 1.

In Phase I, two ceramic shroud systems were evaluated in the initial design phase. The two ceramic shroud systems were as follows: 1) zirconia (ZrO_2) plasma sprayed onto structural metal segments and 2) porous boron nitride/silicon carbide/silicon rub layer bonded to solid, hot-pressed silicon carbide which is mechanically held by metal holders. The zirconia shroud system was selected for further developments based on laboratory testing of the two systems. Laboratory evaluations of the two systems consisted of the following: cold particle erosion, hardness, bond strength, metallography, and thermal shock. The SiC ceramic shroud design was dropped from consideration due to inadequate hot gas erosion resistance.

Phase II consisted of continued evaluation of the plasma sprayed zirconia shroud system selected in Phase I. Various bond and top coat chemistries were studied. The Ni 22Cr 10Al 1Y bond coat composition was selected based on prior General Electric oxidation testing and specific data found in the literature. Also, yttria stabilized zirconia was determined to be superior to magnesia stabilized zirconia based on phase stability and densification during furnace exposure, cold particle erosion, room temperature rub, tensile bond, and thermal fatigue. Thermal shock testing was conducted to compare ZrO_2-$8Y_2O_3$ and ZrO_2-$6.2Y_2O_3$ top coat compositions. Based on power sprayability and results of thermal shock testing, the ZrO_2-$8Y_2O_3$ composition was selected. In addition to selected a zirconia composition, CF6-50 engine testing was conducted to evaluate four shroud configurations. Wire mesh and superpeg configurations were found to be better than the standard CF6-50 peg array designs. A

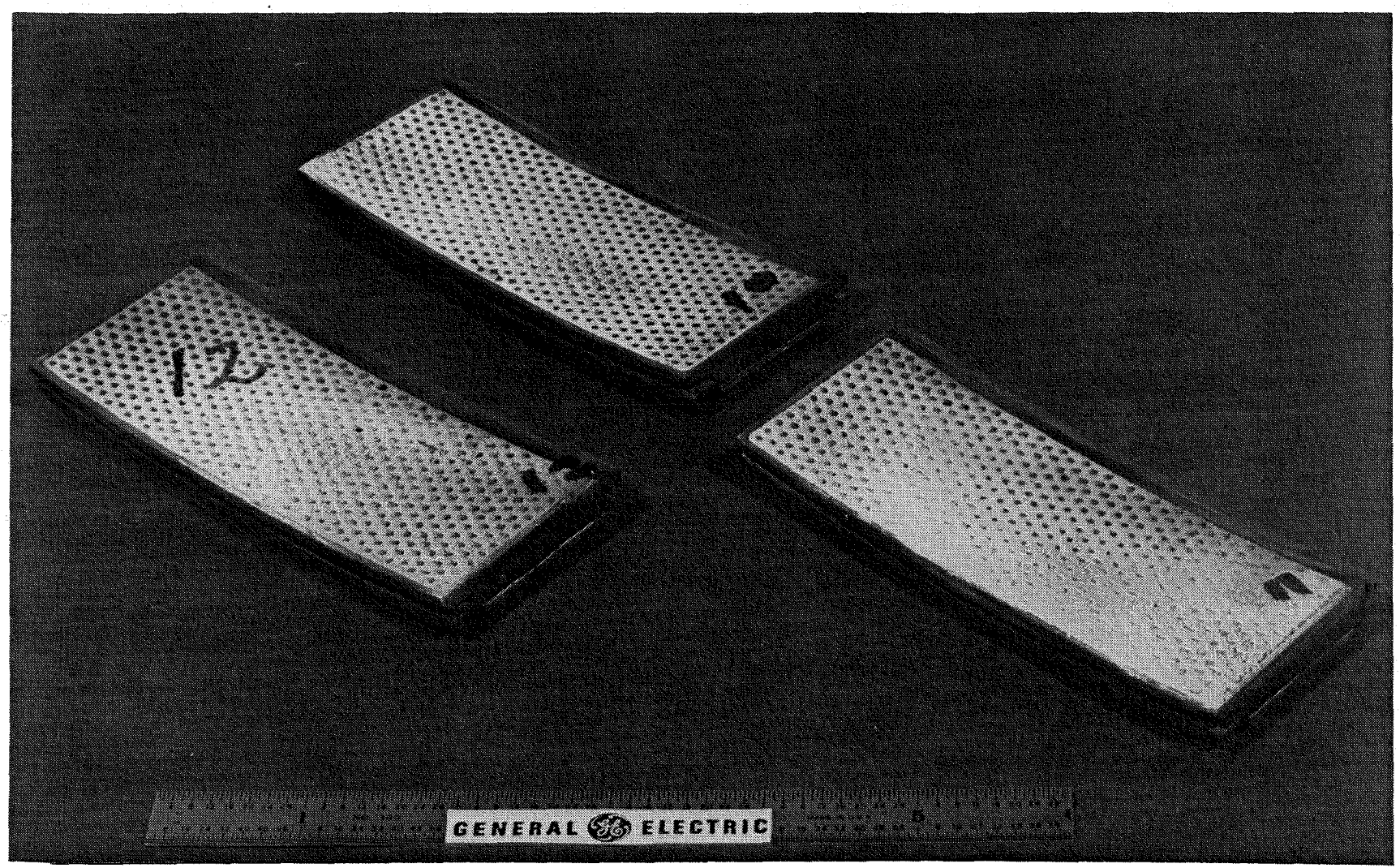

Figure 1. Ceramic Shrouds After Successful CF6-50 Engine Testing

second CF6-50 engine test was conducted to compare the superpeg and wire mesh shroud configurations. The superpeg shroud was selected as prime ceramic shroud configuration for the E^3 engine based on these test results. Also in Phase II studies were conducted on shroud process reproducibility of the superpeg shroud configuration. An automatic spray technique was developed for use with a rotating drum shroud holders. Phase II laboratory studies and CF6-50 engine test led to the selection of the superpeg shroud designs, ZrO_2-$8Y_2O_3$ as the top coat, and the identification of spray process parameters. Component testing was conducted as an integral part of Phases II and III.

Phase III was concerned primarily with development of a suitable non-destructive examination (NDE) technique to detect flaws in zirconia shrouds. Two techniques, holographic and infrared inspection, were evaluated. Holographic inspection was not selected due to inconsistent results, while the infrared technique was selected based on analysis of ceramic coated panels.

In Phase IV, a total of 52 zirconia coated stage 1 HPT (High Pressure Turbine) shrouds were fabricated for E^3 core and ICLS (Integrated Core and Low Pressure Spool) testing. The shrouds were of superpeg configuration with ZrO_2-$8Y_2O_3$ triplex coating system. The shrouds were fabricated in two separate lots. Two shrouds from Lot 1 were successfully tested for 1000 thermal cycles on the Lynn thermal shock rig. The remaining shrouds currently await engine testing.

II. INTRODUCTION

Gas turbine performance is greatly influenced by blade tip-to-shroud gas leakages, along with shroud cooling air requirements. Such blade tip-to-shroud leakage can be minimized between the two components. Considerable work has been done to reduce clearances by using acceptably abradable shroud linings to prevent blade tip wear. Further performance improvements can be achieved by reduction of the cooling air, but subjects the shroud material to higher temperatures. Hence, there exists a need for more stable shroud materials which can withstand temperatures in excess of 1370° C (2500° F). Stable oxide ceramics, such as zirconia (ZrO_2) flowpath surfaces, when suitably secured to plasma sprayed bond interfaces offer unique HPT shroud capabilities. These ceramic materials at temperatures above 1375° C (2500° F) produce dimensionally stable structures, can operate with less cooling air, can provide thermal shielding of underlying structures, are lighter in weight than conventional metallic shrouds, and have lower life cycle costs than solid shroud design. For most ceramic shroud systems, however, General Electric and NASA experience has shown that a key factor in assessing the potential of ceramic systems is their thermal shock resistance[1]. As a consequence, thermal shock characteristics were extensively studied.

The objective of this effort was to identify, fabricate, and test a high temperature shroud material for HPT Stage 1 application in the Energy Efficient Engine (E^3). The program has been carried out in four phases. In Phase I, candidate materials were identified from a ranking procedure incorporating selective type screening tests. In Phase II, process procedure were developed in an iterative manner, then specimens and shroud elements produced were evaluated by laboratory and rig tests. In Phase III, ZrO_2-Y_2O_3 ceramic shrouds were fabricated, inspected with developed NDE procedures, and evaluated in full scale component and factory engine tests. Finally, in Phase IV the ZrO_2-$8Y_2O_3$ superpeg shrouds for the E^3 engine were fabricated by the developed automatic spray process, proof tested, examined by NDE, and accepted for engine testing.

III. SELECTION OF CERAMIC SHROUD CANDIDATE - PHASE I

The initial phase of the ceramic shroud development program consisted of a review of alternative design-material systems and an assessment of their durability characteristics in meeting engine test requirements. Two basic ceramic shroud concepts were evaluated in the initial design phase: zirconia (ZrO_2) plasma sprayed onto metal segments, Figure 2, and porous boron nitride/silicon carbide/silicon rub layer bonded to solid, hot-pressed silicon carbide, mechanically held by metal holders, Figure 3. The zirconia shroud system was determined to be superior based on the results of screening tests and was therefore selected for further development in Phases II and III.

Laboratory testing was conducted to assess pertinent gas-path seal characteristics related to each shroud system. The ZrO_2 and SiC ceramic shrouds were evaluated by metallography, hardness, cold particle erosion, tensile bond, and thermal shock testing. Mach 1.0 gas oxidation/erosion on the SiC ceramic along with other pertinent testings were conducted in part, and reported under a separate efforts[2]. The SiC shroud approach was dropped from consideration due to inadequate hot gas erosion resistance of the boron nitride/silicon carbide/silicon rub layers at expected operation temperatures. Figure 4 shows the severe erosion of the silicon carbide specimens which occurred during hot gas erosion testing at 1315° C (2400° F) and 1260° C (2300° F).

The zirconia plasma sprayed ceramic was found to exhibit adequate shroud chracteristics based on preliminary examinations and evaluations. Further efforts on the plasma sprayed zirconia were conducted in Phases II and III.

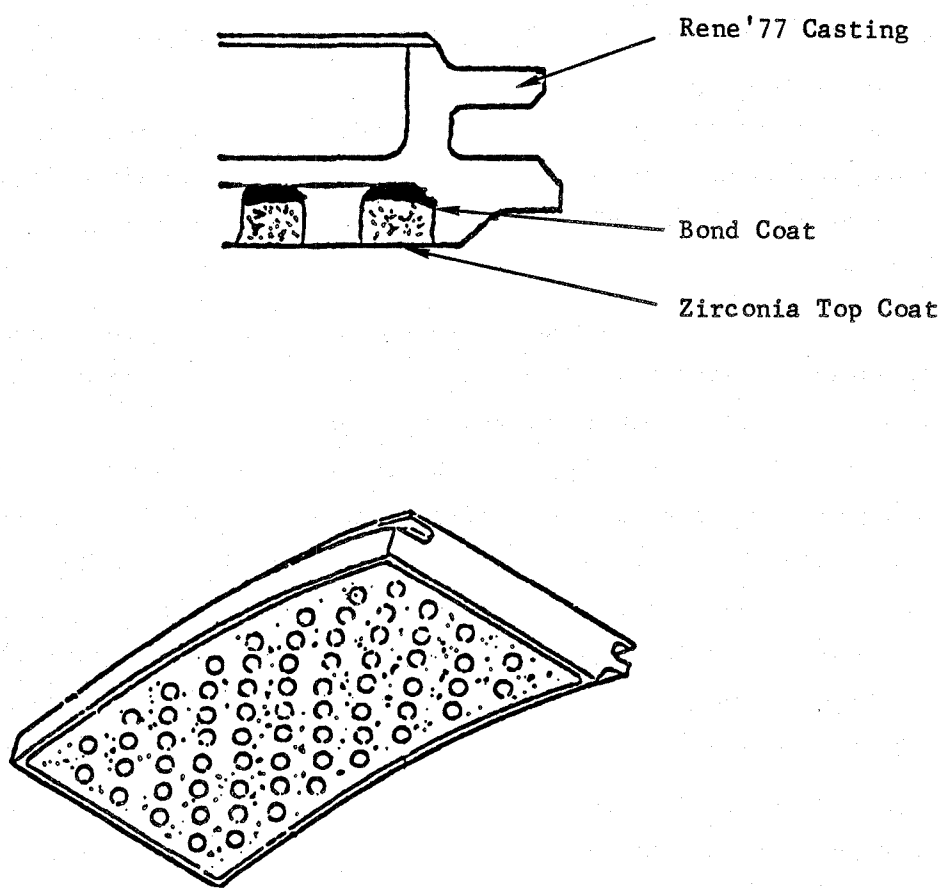

Figure 2. Zirconia Ceramic Shroud Design Concept

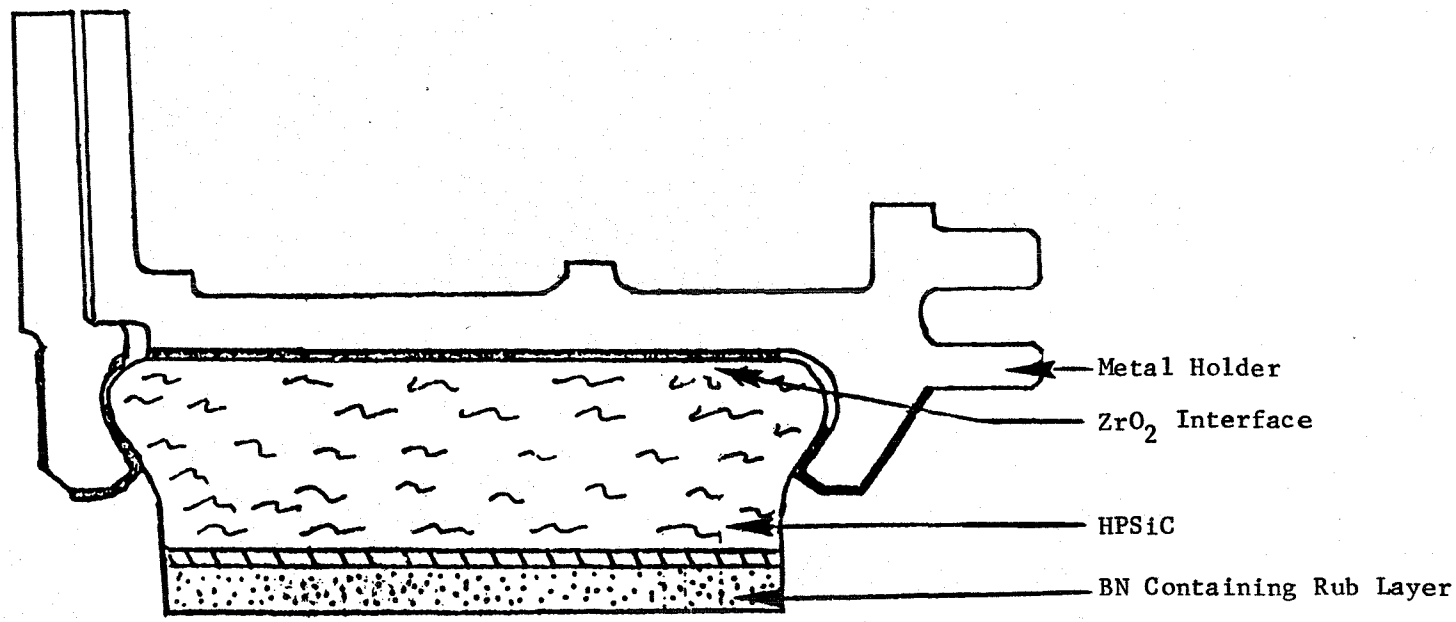

Figure 3. Hot Pressed Silicon Carbide Shroud Design Concept

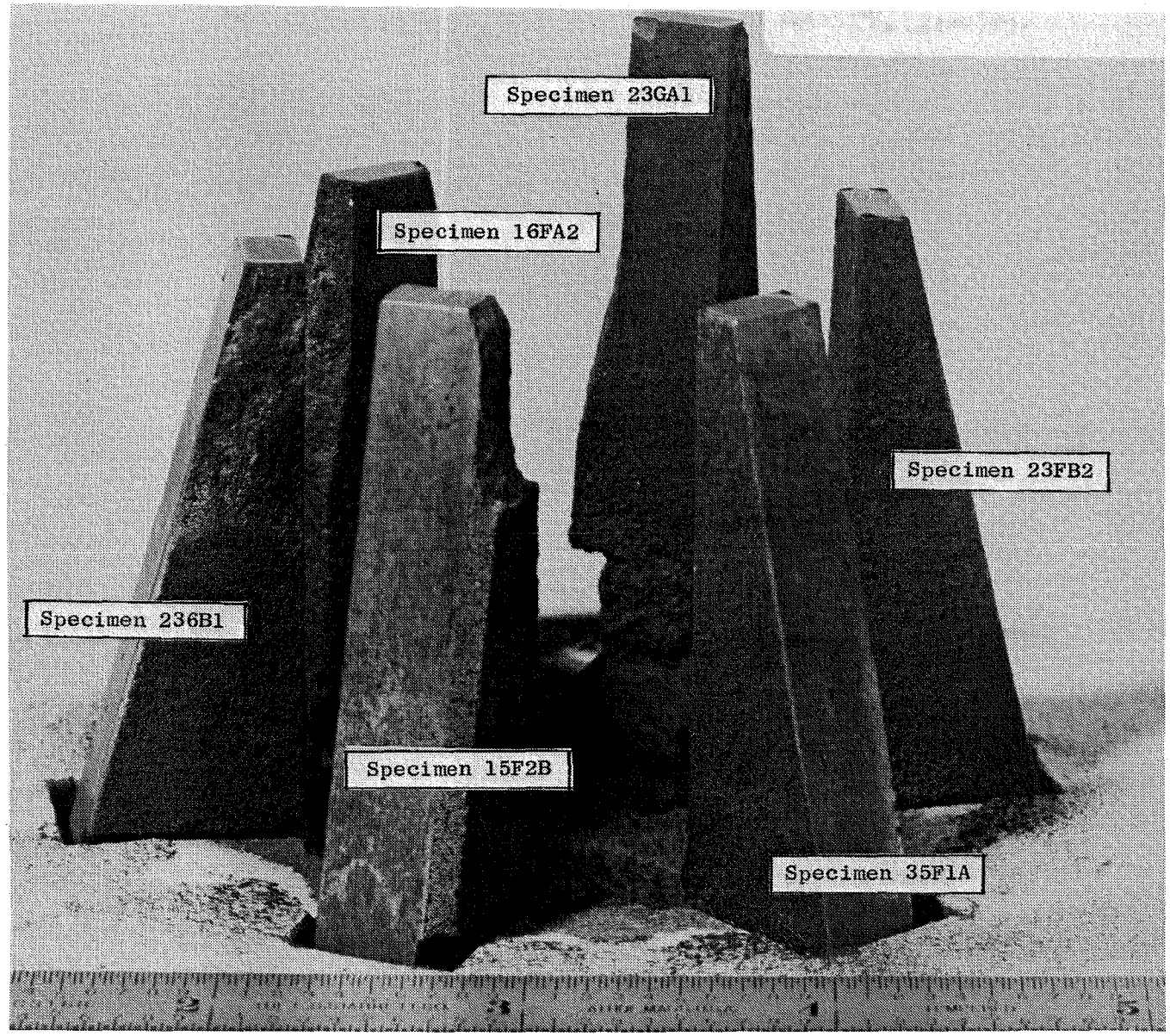

Figure 4. Mach 1.0 Gas Oxidation/Erosion SiC Specimens in Holder After 8 Hours at 1315°C (2400°F) and 20 Hours at 1260°C (2300°F)

IV. DEVELOPMENT OF A CANDIDATE SHROUD SYSTEM - PHASE II

In this phase, further evaluation of plasma sprayed ZrO_2 shroud systems was conducted with particular emphasis directed toward evaluation of thermal fatigue, erosion resistance, and thermal stability of the ZrO_2 flowpath coating. Included in this study was a comparison of different ZrO_2 compositions. The approach used in Phase II was: 1) characterize and determine thermal stability of candidate ZrO_2 coatings, 2) make a chemistry selection based on thermal stability and thermal fatigue, 3) conduct thermal shock rig tests of a selected chemistry and configuration (selection of chemistry and configuration to be based on CF6-50 engine test results), and 4) evaluate the basic spray process and controls, and reproducibility.

Eight coating systems (four ZrO_2 top coat and two bond coat combinations) were evaluated by collecting and analyzing specific data found in technical literature. The candidate top coats and bond coats are listed in Table I. The two bond coat compositions, Ni-22Cr-10Al-1Y and Ni-16.4Cr-5.1Al-0.15Y, were reviewed with respect to their oxidation resistance since permeation of oxygen to the bond coat through the ZrO_2 top layer is expected. The Ni-22Cr-10Al-1Y bond coat was found more oxidation resistant than Ni-16.4Cr-5.1Al-0.15Y based on oxidation studies on NiCrAlY of various compositions[3], and was selected for use in this study. The number of ZrO_2 compositions to be characterized and tested in preliminary thermal shock tests was reduced from four to two on the basis of published work by NASA[4] on the thermal shock behavior of these coatings. This NASA effort has shown the superiority of ZrO_2-6.2Y_2O_3 over ZrO_2-12Y_2O_3. The ZrO_2-3.4MgO partially stabilized zirconia was eliminated because this composition is essentially monoclinic zirconia and the large volume change (up to 9 percent) associated with the monoclinic-to-tetragonal phase transformation is a concern in thermal shock behavior. The prior work at General Electric on high pressure turbine shrouds had incorporated the ZrO_2-24MgO ceramic. The rig tests conducted had shown promising results with this ZrO_2-24MgO shroud system. It should be noted that additives such as MgO and Y_2O_3 to ZrO_2 are used to stabilize the cubic phase and minimize other crystallographic tranformations.

Table I. Candidate Compositions Evaluated in Phase II.

Top Coat Compositions*:

ZrO_2-6.2Y_2O_3

ZrO_2-12Y_2O_3

ZrO_2-3.4MgO

ZrO_2-24Mgo

Bond Coat Compositions*:

Ni - 16.4 Cr - 5.1 Al - 0.15 Y

Ni - 22 Cr - 10 Al - 1 Y

*Weight Percent

The two zirconia composition candidates selected for further tests with Ni-22Cr-10Al-1Y bond coat were. ZrO_2-6.2Y_2O_3 and ZrO_2-24MgO.

The evaluation consisted of the following:

1. Phase stability, microstructure and sintering behavior at 1260° C (2300° F) and 1371° C (2500° F) as a function of time for up to 500 hours.

2. Thermal shock resistance where shroud specimens were cycled from 1371° C (2500° F) to about 204° C (400° F). In this test a temperature gradient of approximately 675° C (1200° F) was maintained through the specimen thickness to simulate engine conditions. Also, following the stability and sintering exposures, the specimens were evaluated for cold particle erosion resistance, room temperature rub-tolerance, and surface hardness.

Figure 5 shows the percent of monoclinic phase as a function of exposure time. The phase stability study showed that the amount of monoclinic phase in ZrO_2-6.2Y_2O_3 increased slightly up to 250 hours of exposure of 1260° C (2300° F) and 1371° C (2500° F), and did not change for exposure up to 500 hours at these temperatures. The ZrO_2-24MgO became fully monoclinic after only 50 hours at 1260° C (2300° F) and continued to be fully monoclinic for exposures up to 500 hours. At 1371° C (2500° F), the amount of monoclinic phase increased slightly upon exposure but did not further change after 50 hours of exposure.

The sintering behavior, of both zirconia chemistries is shown by densification in Figure 6. The as-sprayed density of ZrO_2-6.2Y_2O_3 was 5 percent less than that of ZrO_2-24MgO. After 500 hours of exposure, ZrO_2-6.2Y_2O_3 sintered 4 percent at 1371° C (2500° F) and 2 percent at 1260° C (2300° F). The ZrO_2-24MgO sintered 5 percent at 1371° C (2500° F) and 4 percent at 1260° C (2300°F).

Figure 7 is a log-linear plot of cold particle erosion resistance of the two zirconias after high temperature exposure. The erosivity factor is a measure of the rate of erosion of a target material subjected to an alumina grit blast. A high value of erosivity factor [sec/mm(sec/mil)] denotes good cold particle erosion resistance. The test data indicates that ZrO_2-6.2Y_2O_3 after exposure time of greater than 10 hours has better cold particle erosion resistance than ZrO_2-24MgO.

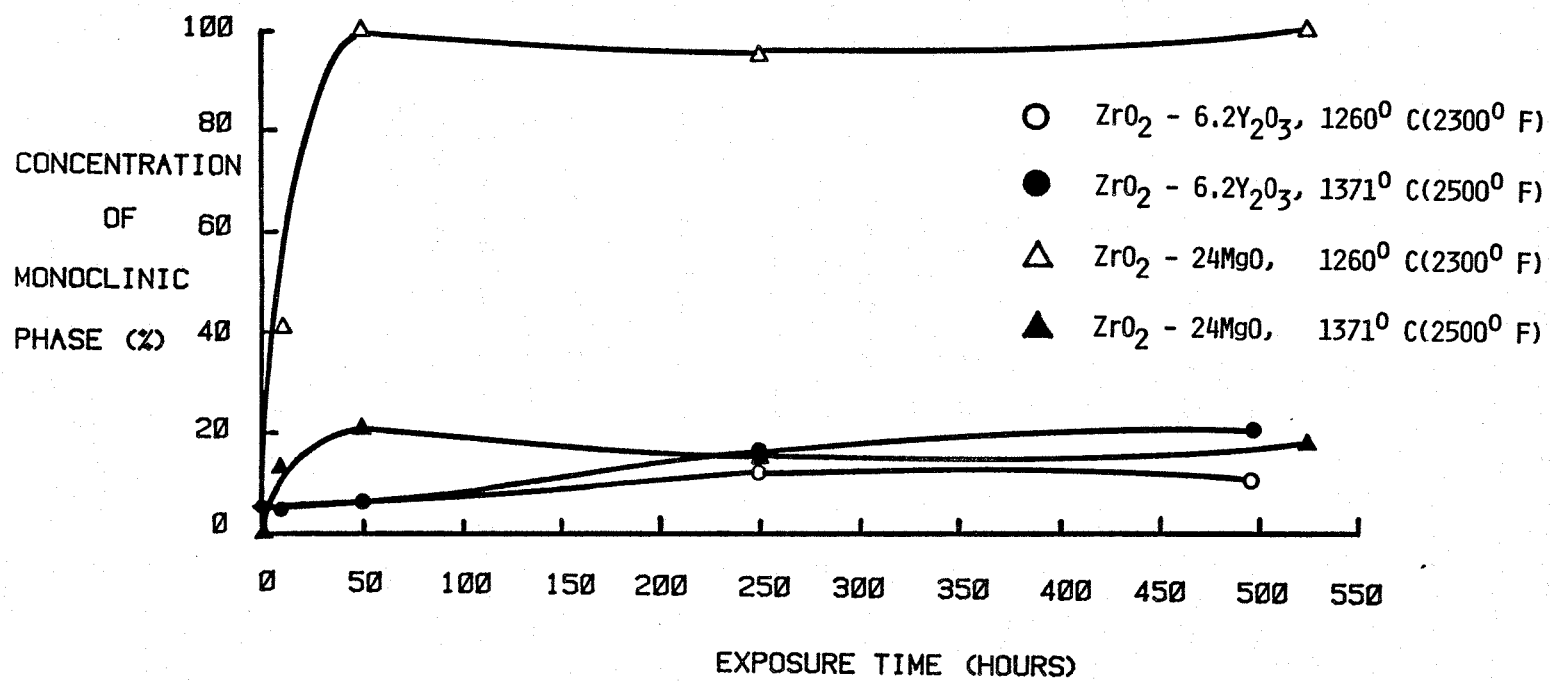

Figure 5. Concentration of Monoclinic Phase vs Exposure Time

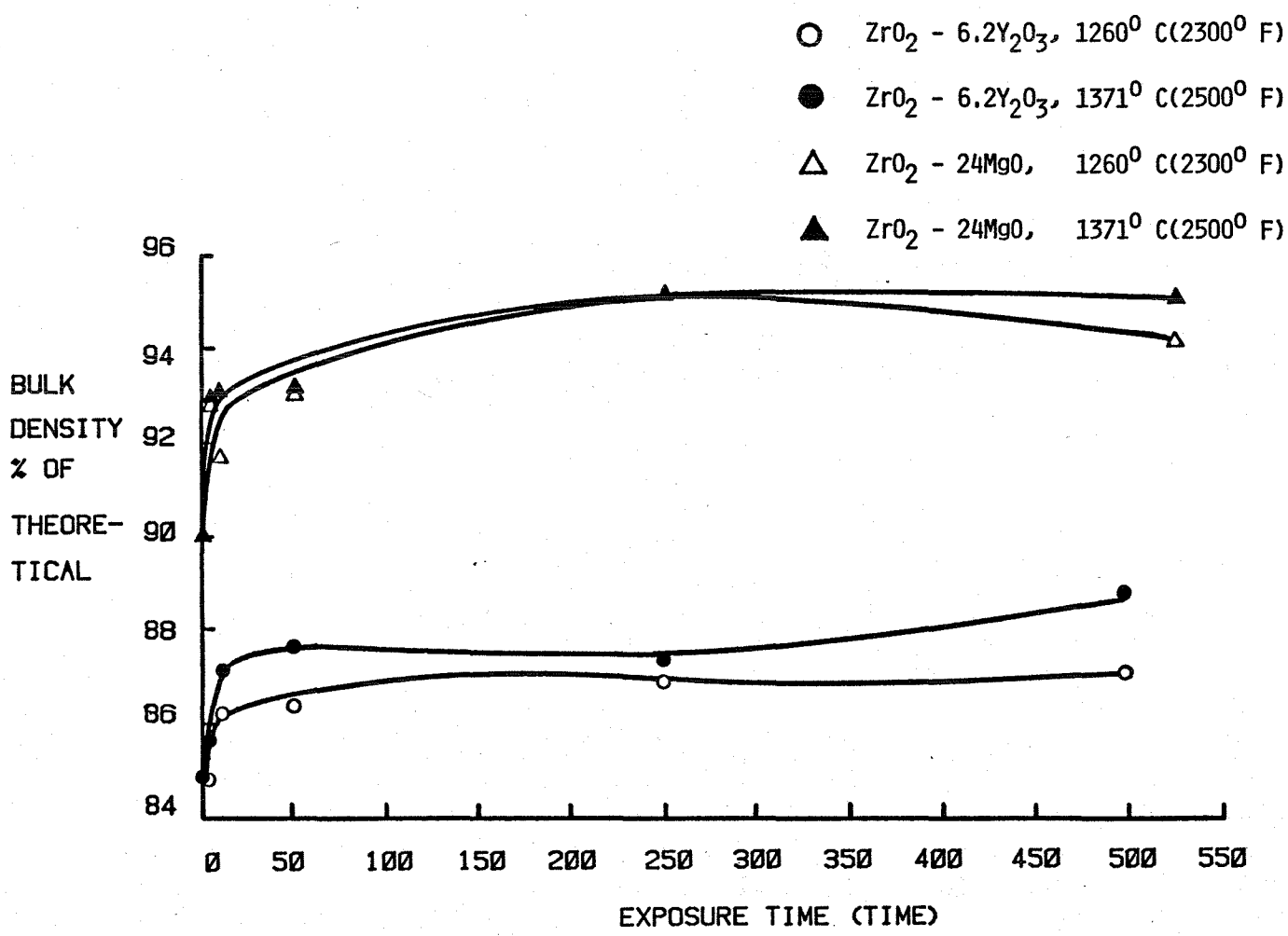

Figure 6. Sintering Behavior

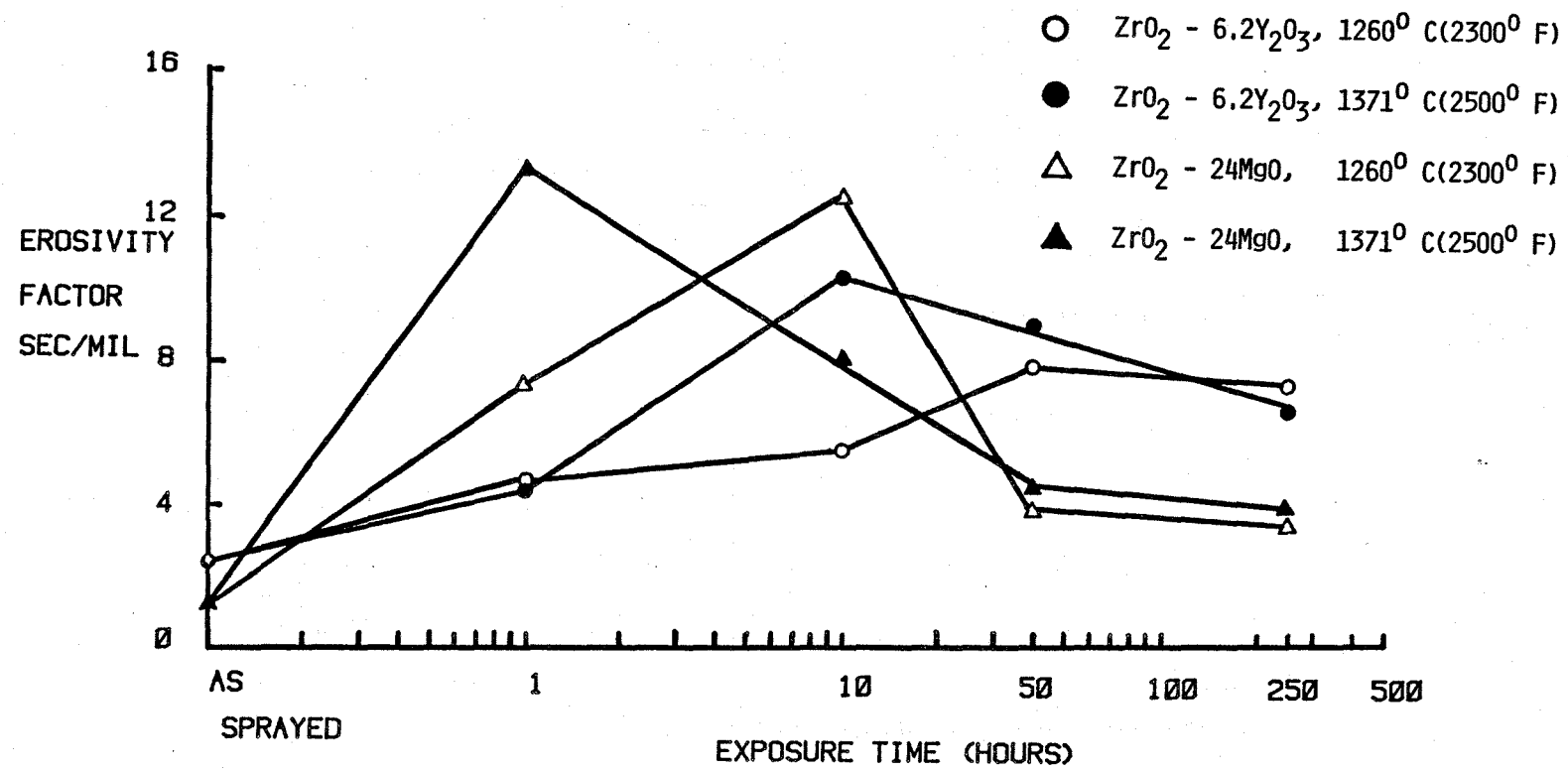

Figure 7. Effect of High Temperature Exposure on Cold Particle Erosion Resistance

Figure 8 presents a log-linear plot of the room temperature abradability behavior as a function of exposure time. In abradability testing, the abradable material is supported on a platform beneath the rotating blade elements. During the test, the blades rotate at 229 sms (750 sfs) with an incursion rate of 0.025 mm/second (1 mil/second) to generate a total incursion of about 0.508 mm (20 mils). The abradability factor is a measure of rub behavior and is given by the equation below:

$$\text{abradability factor} = \frac{\text{incursion depth} - \text{blade wear}}{\text{blade wear}}$$

Higher values of abradability factor indicate better room temperature rub behavior, i.e., less blade wear. One shortcoming of this formula is the unaccountability for any blade metal transfer to the coating surface during rub (scabbing). No clear trends could be established from the data in Figure 8 due to scabbing and blade distress which occurred. The abradability of zirconia coatings seems to decrease after 250 hours exposure, most probably due to densification of the coating. For both chemistries, the specimens could not be rubbed for more than 5 seconds [incursion rate of 0.0254 mm (0.001 inch/second)] due to scabbing and blade distress. In conclusion, the type of ZrO_2 (MgO, Y_2O_3) used was not shown to be a significant variable in wear chemistries.

Room temperature tensile bond testing to determine cohesive strength was conducted on 2.54 cm (1 inch) diameter discs. Tensile tab segments of 2.54 cm (1 inch) were bonded to the ceramic surface and the substrate and pulled to failure at 0.127 mm/min (0.005 inch/min). The change in cohesive strength versus exposure time is shown in Figure 9. In general, these results show that the cohesive bond strength decreases with exposure time. The effect of exposure times on hardness was also determined. The hardness scale was selected as R15Y which was a 1.27 cm/min (0.5 inch) diameter steel ball indenter and a load of 15 kg (33 lbs). Figure 10 shows that the two zirconias have similar room temperature surface hardness.

In the thermal fatigue resistance evaluation, both ZrO_2-Y_2O_3 and ZrO_2-MgO shroud segments were cycled from 1388° C (2530° F) to less than 204° C (400° F)

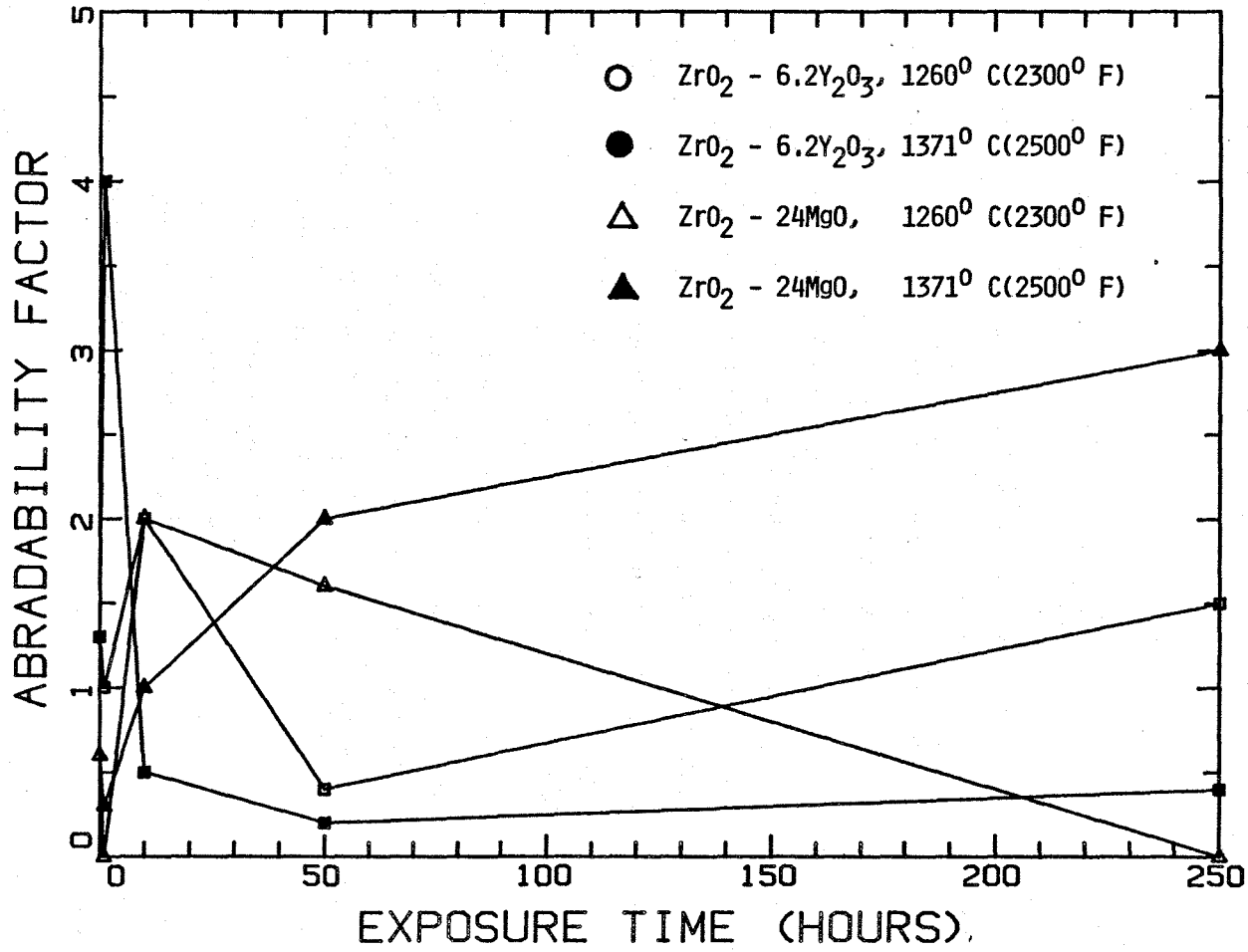

Figure 8. Effect of High Temperature on Abrasion Resistance

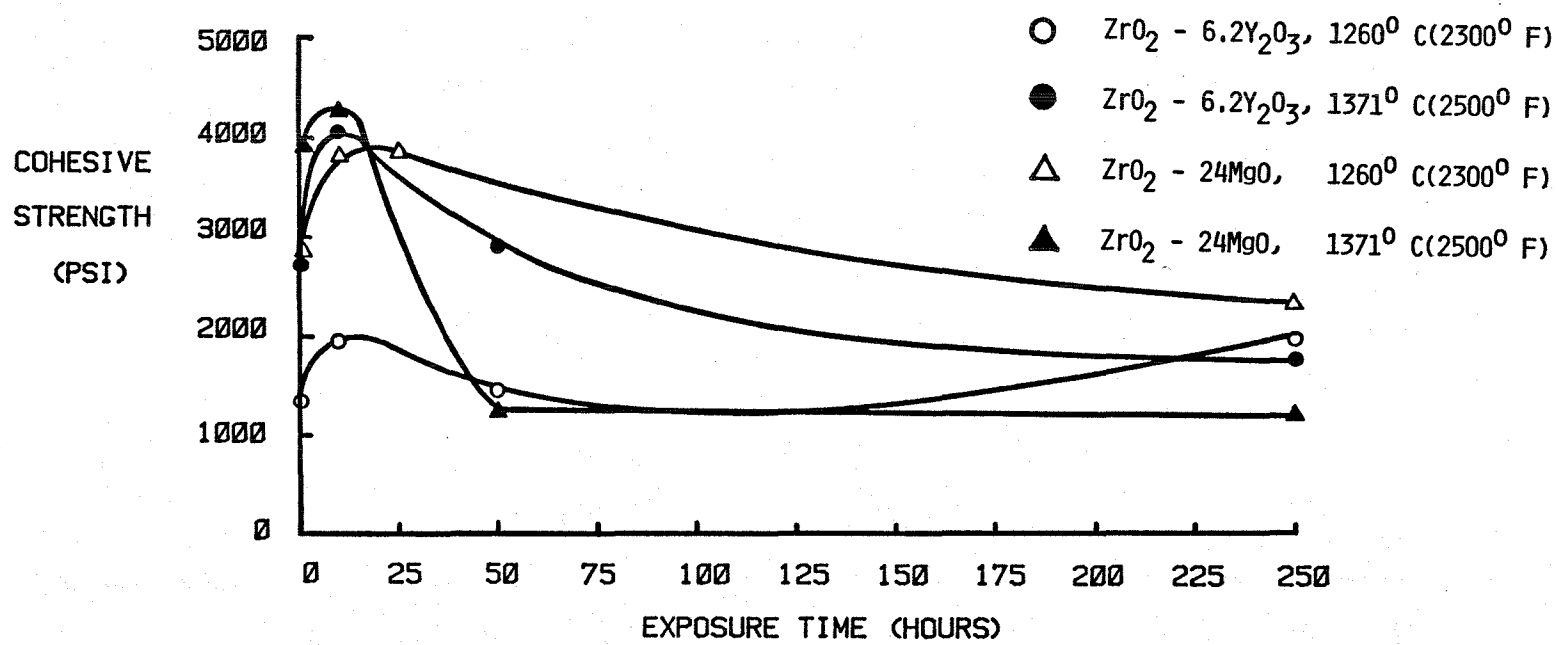

Figure 9. Effect of High Temperature Exposure on Cohesive Strength

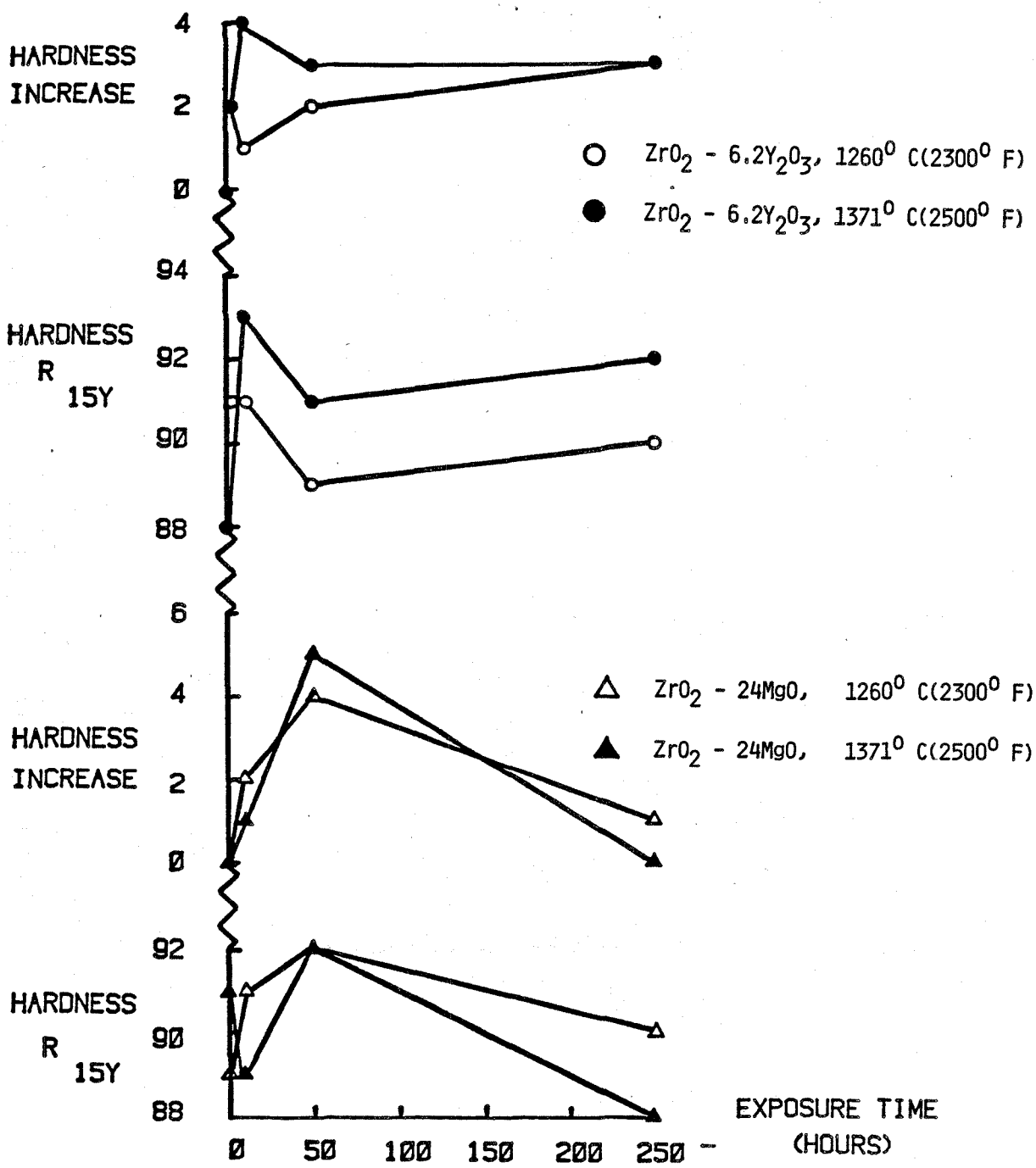

Figure 10. Effect of High Temperature Exposure on Surface Hardness

for 50, 200, 500, and 1000 cycles. The thermal shock tests apparatus is pictured in Figure 11. Separate shroud segments were used for 50, 200, and 500 cycles. Figure 12 shows the shrouds after 500 cycles. The 500-cycle specimens were then tested for an additional 500 cycles to accumulate 1000 cycles. The ZrO2-6.2Y_2O_3 specimens cycled for 50, 500, and 1000 cycles contained no mud flat surface cracking, no cracks along the edges, but did have some corner and edge clipping (probably related to ZrO_2 overspray). The ZrO_2-24MgO specimens cycled for 50, 500, and 1000 cycles did show mud flat surface cracking as well as an edge crack along the perimeter of the specimen at the ZrO_2-24MgO bond interface which grew wider with increased number of cycles. No separation of the ZrO_2-24MgO took place, however. On the other hand, the ZrO_2-6.2Y_2O_3 specimen which cycled for 200 cycles showed some mud flat surface cracking and edge cracking, while the 200-cycle ZrO_2-24MgO specimen contained no mud flat cracking although it did contain some edge cracking. This lower than expected thermal shock behavior after 200 cycles for the ZrO_2-6.2Y_2O_3 specimen was anomolous to what had occurred previously. A repeat of this experiment using additional shrouds showed ZrO_2-6.2Y_2O_3 shrouds to be superior to ZrO_2-24MgO.

The results of the characterization study and thermal fatigue resistance evaluation can be summarized as follows:

- ZrO_2-6.2Y_2O_3 composition is essentially stable after 500 hours of exposure with respect to density, amount of monoclinic phase present, and microstructure. Phase transformations occur in the ZrO_2-24MgO composition.
- ZrO_2-6.2Y_2O_3 is more stable crystallographically.
- ZrO_2-6.2Y_2O_3 sinters slightly less than ZrO_2-24MgO.
- ZrO_2-6.2Y_2O_3 is superior or equal to ZrO_2-24MgO in cold particle erosion resistance, cohesive strength, and surface hardness.
- No significant difference could be determined in room temperature rub behavior.
- ZrO_2-6.2Y_2O_3 is superior to ZrO_2-24MgO in thermal fatigue resistance.

Additional thermal shock and laboratory evaluation was conducted to compare ZrO_2-MgO and ZrO_2-6.2Y_2O_3 shrouds. A total of eleven shrouds of the wire

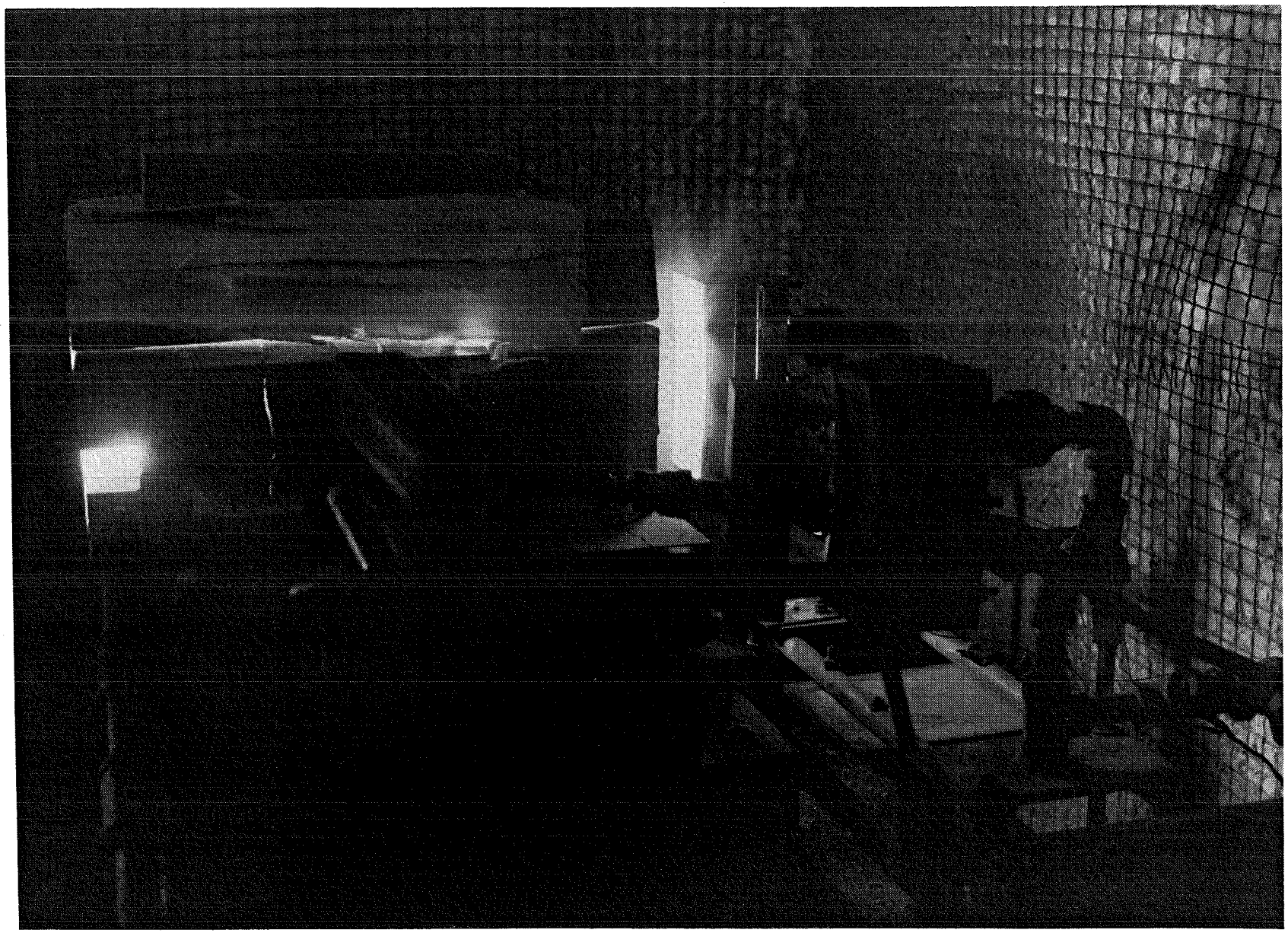

Figure 11. Thermal Shock Test Rig for Ceramic Shroud Testing

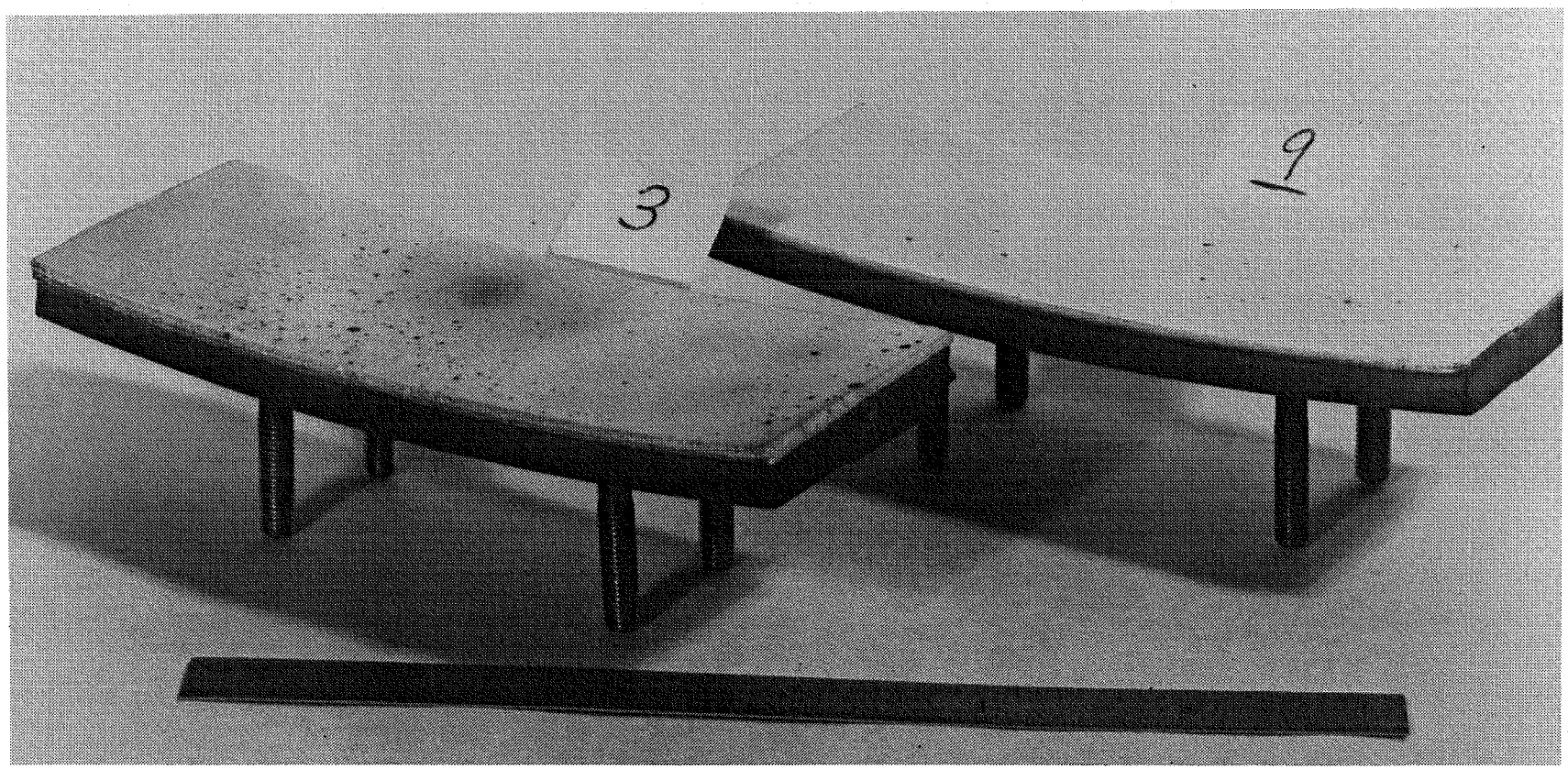

Figure 12. Ceramic Shroud Segments after 500 Test Cycles

configuration were fabricated for evaluation. The wire mesh configuration of these shrouds consisted of the following: Genaseal on the René 77 casting, IN600 wire mesh, NiCrAlY bond coat, NiCrAlY/ZrO_2 blend coat, and zirconia top coat. Five shrouds had ZrO_2-24MgO top coat, three had ZrO_2-6.2Y_2O_3 standard density top coat, and three had ZrO_2-6.2Y_2O_3 low density (75% dense) top coat. The process to deposit 75% dense ZrO_2-6.2Y_2O_3 had been developed earlier during this program. Six of these shrouds were used in the thermal shock testing to be described next, while the remainder were used in quality control checks.

Thermal shock testing of these shrouds was conducted at General Electric's facility in Lynn, Massachusetts, as shown previously (Figure 11). The zirconia flowpath surface was maintained at 1400° C (2550° F) while the back was cooled to 727° C (1340° F) in the heating station. The sample was alternated between the afore-described heating station and a cooling station which cooled the entire shroud to approximately 204° C (400° F). The specimens were cycled 10 times/hours, three minutes heating and three minutes cooling per cycle. Two 1000 cycle tests were conducted with two shroud segments in each test. The first test thermal shocked shroud segments containing ZrO_2-24MgO heat treated to transform the ZrO_2 and standard density ZrO_2-6.2Y_2O_3. The second test thermal shocked shroud segments containing ZrO_2-24MgO with no heat treatment and low density ZrO_2-6.2Y_2O_3. All four of these specimens completed the 1000 cycle test with no apparent distress. A 3000 cycle test was then initiated with ZrO_2-6.2Y_2O_3 and ZrO_2-24MgO (heat treated). The ZrO_2-24MgO shroud specimen developed a 0.635 cm (1/4 inch) diameter spall at 2869 cycles, while the ZrO_2-6.2Y_2O_3 shroud completed 3000 cycles without incident, Figures 13 and 14. The ZrO_2-6.2Y_2O_3 coating system was selected based on thermal shock test, phase stability studies, and ease of coating application.

A CF6-50 engine test was performed to compare four shroud design configurations, shown in Figure 15, to select one design for further development. These configurations were standard support peg array, half-height buried peg array, wire mesh, and fine array of circular pegs ("superpeg"). Details on engine testing are contained in Appendix A and are also briefly covered below. Eight magnesia stabilized zirconia shrouds were SMP (Systems Mechanical and Performance) tested in August 1979. Total running time was 65:22 hours, with

Figure 13. ZrO_2 - 24 MgO Coated Wire Mesh Shroud Segment After 2689 Thermal Shock Cycles

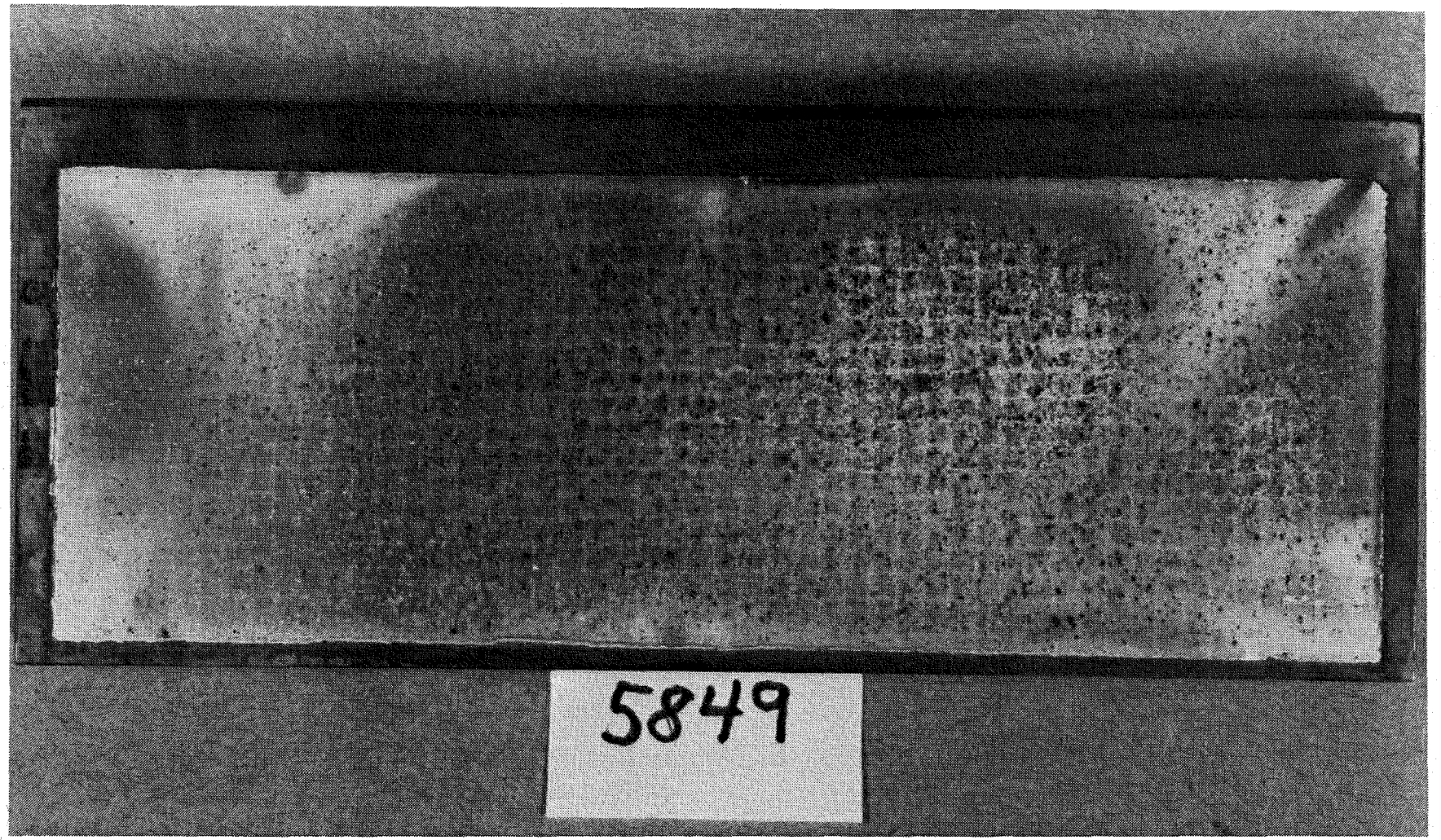

Figure 14. ZrO_2 - $6.2Y_2O_3$ Coated Wire Mesh Shroud

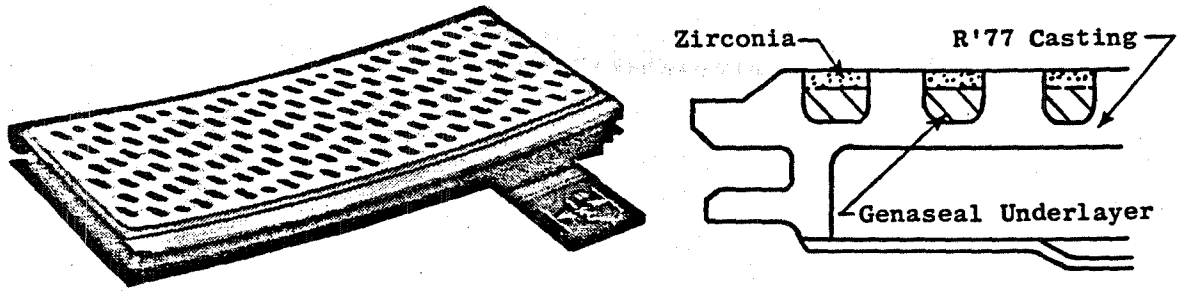

Configuration 1 - Metal Pegs Through Zirconia

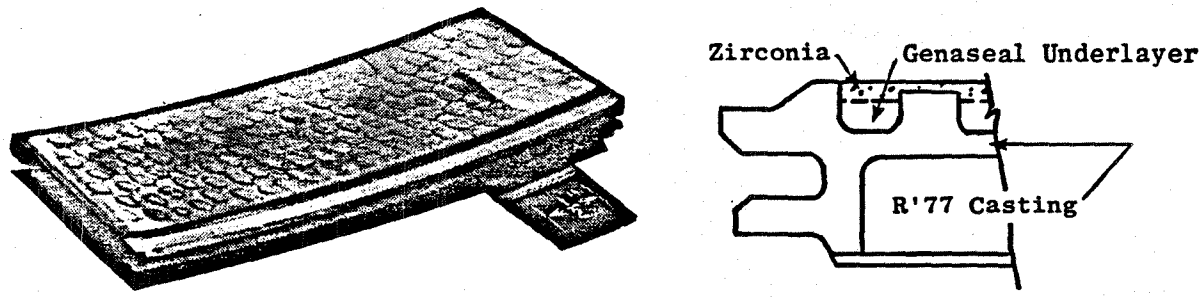

Configuration 2 - Short Metal Pegs Recessed Below Surface of Zirconia

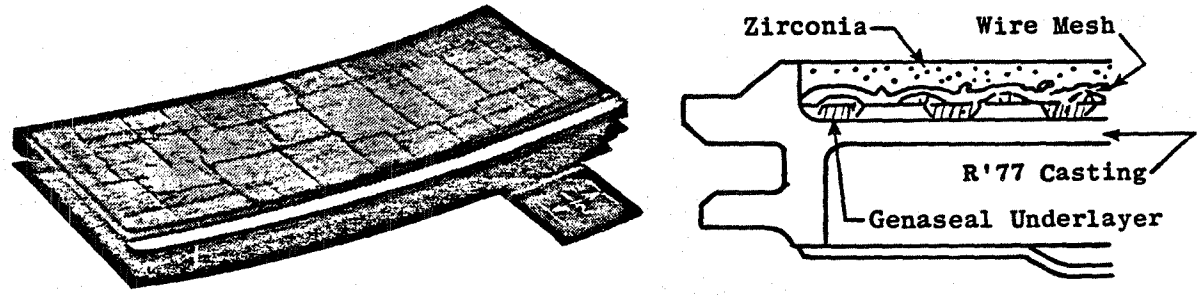

Configuration 3 - Wire Mesh at Bottom of Zirconia Layer

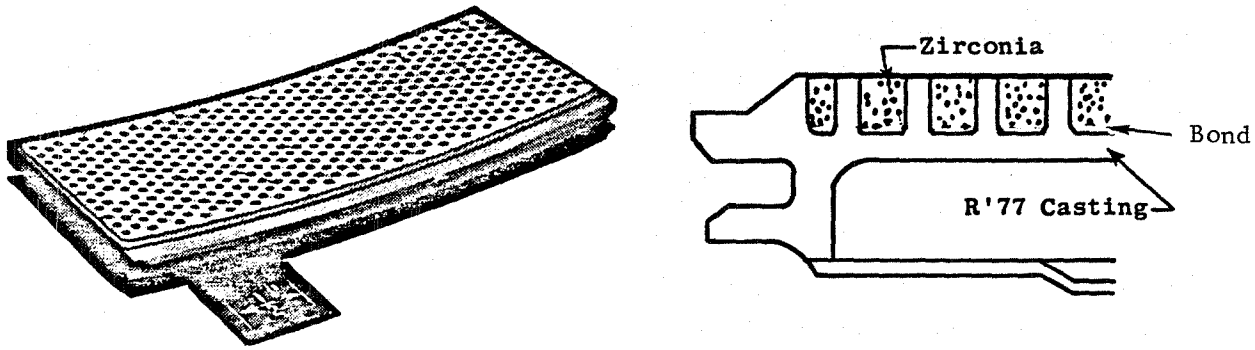

Configuration 4 - Super Peg (Closely Spaced Round Pegs) Design, No Genaseal Underlayer

Figure 15. ZrO_2 - 24MgO HP Turbine Shrouds for CF6-50 Engine Test

5.07 hours at the turbine rotor inlet temperature in the range of 1371° C (2500° F) to 1400° C (2550° F) (maximum). Figure 16 shows the four different shroud configurations after engine testing. The wire mesh shrouds showed no distress, while the superpeg shrouds exhibited minor spalling of zirconia top coat at the edges which did not have a full row of pegs. One shroud from both the remaining designs of the standard support peg array and of the half-height buried peg array, showed unacceptable spallation of the zirconia top coat. The wire mesh and superpeg designs were deemed best of those tested and both were selected for further development and evaluation.

A process control study was conducted to determine parameters for brazing the wire mesh anchoring system to the shroud backing. The proper amount of braze alloy required and the braze wetting characteristics were determined by microscopic and visual evaluations. Four wire mesh shrouds were utilized for this study. Top coat delamination was noted during this study and attributed to power characteristics, such as fine particle size and shape, which probably inhibited power flow during spray. The difficulty with power spraying necessitated the need for a more uniform, free-flowing zirconia powder. Metco Company's ZrO-Y_2O_3 was identified and approved as an alternate powder source based on NASA and General Electric experience. The Metco powder was ZrO_2-$8Y_2O_3$ composition rather than ZrO_2-$6.2Y_2O_3$ as was previous used. Six wire mesh shrouds were fabricated; four with powder from the alternate source and two with powder from the original vendor. Based on sprayability of powder and comparative thermal shock testing for 1000 cycles, the ZrO_2-$8Y_2O_3$ powder was selected over the previously used ZrO_2-$6.2Y_2O_3$ powder.

In November of 1980, a second CF6-50 factory engine test was conducted to compare the wire mesh and superpeg shroud designs. Ten shrouds were fabricated and tested for 625 "C" cycles. Based on the post-test analysis, the superpeg shroud was selected as the ceramic shroud configuration for E^3 Core and the ICLS (Integrated Core and Low Pressure Spool) engine testing. The wire mesh design, which did not perform as well as the superpeg design, was deleted from the program.

A shroud reproducibility study was then conducted for the superpeg shroud configuration. Hast X panels were EDM'ed to produce the superpeg

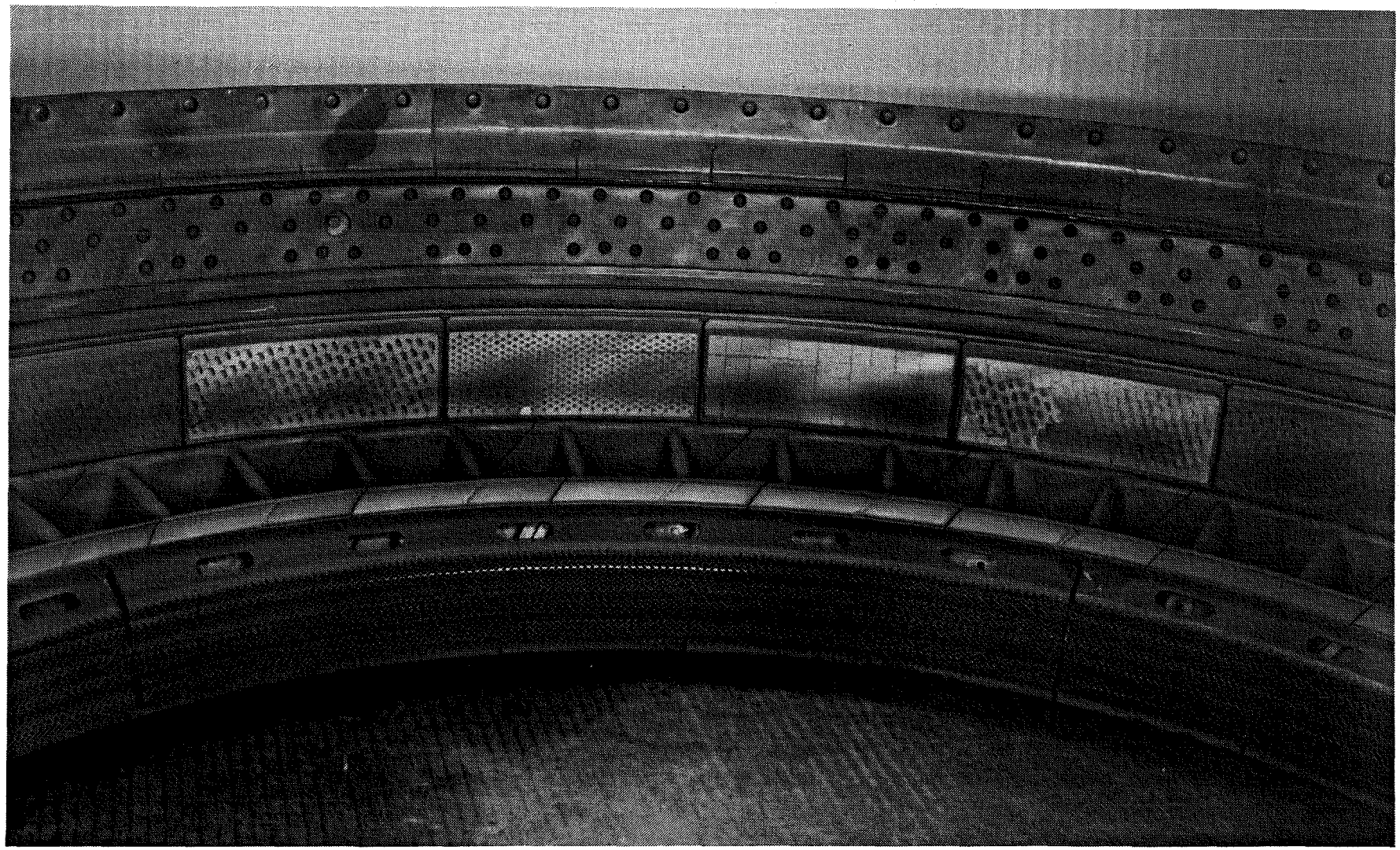

Figure 16. Four Shrouds With Different Design Configurations After 0.7 Hours CF6-50 Engine Testing

configuration. Microscopic evaluation was used to evaluate four spray variations. From this study a technique to minimize shadowing due to sprayed powder accumulation on peg tips was developed. In addition, the automated rotating drum process procedure was developed and incorporated (Figure 17). This automatic spray gun manipulation, rather than the previously used hand spray technique, produced a greatly improved product. A 1000 cycle thermal shock test was conducted as part of the shroud reproducibility study. Hast X panels were brazed into CF6-50 shroud castings and coated with ZrO_2-$8Y_2O_3$. Thermal shock testing of the brazed Hast X panels with coating led to early shroud failure due to debonding of the braze joint between the Hast X superpeg insert and René 77 substrate. Shrouds containing cast-in-pegs would not fail by this braze debond mechanism.

The work in this phase resulted in the selection of the superpeg shroud design, ZrO_2-$8Y_2O_3$ as the top coat, and the identification of the scaled-up process spray parameters.

A third CF6-50 engine test was conducted with superpeg and wire mesh ceramic shroud design. After completion of a planned 750 "C" cycles test the superpeg design shrouds were found to be in good condition and superior to the wire mesh design shrouds.

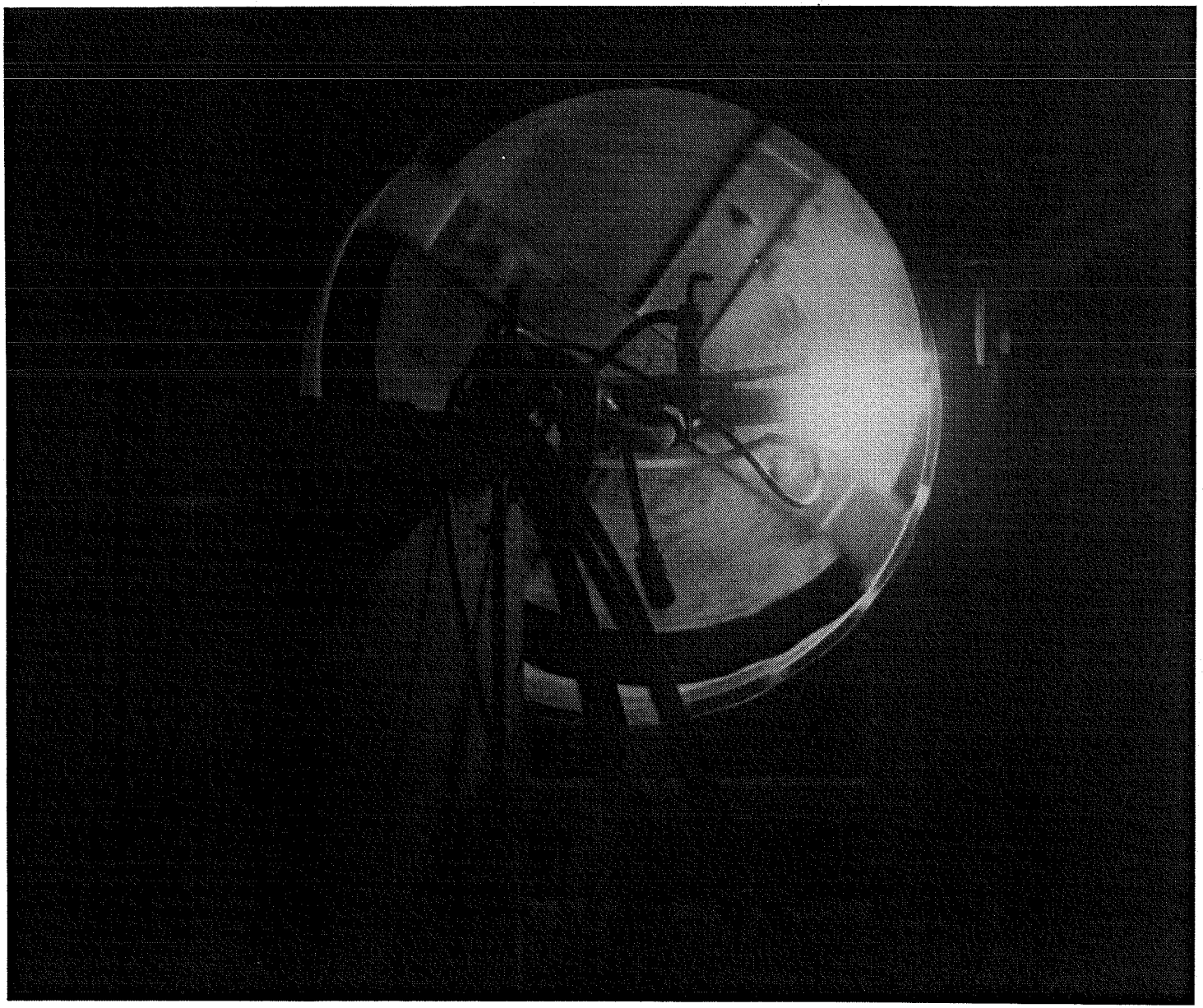

Figure 17. Automated Plasma Spray Facility for Manufacturing Ceramic Shrouds

V. COMPONENT TEST HARDWARE - PHASE III

This phase was concerned primarily with identification and subsequent development of a non-destructive examination (NDE) technique to inspect E^3 component test hardware. A particular goal of the inspection technique was to detect unbonded regions, cracks, or delaminations within the coating system. An infrared technique was selected based on initial analysis of ceramic coated panels containing known defects. In the course of this evaluation, a holographic NDE technique was also evaluated but yielding inconsistent results.

The infrared inspection technique utilized for ceramic shrouds consisted of isothermally heating the shrouds in an oven, removing the shroud from the oven, placing it in a fixture, and photographing the thermographic pattern of the shroud flowpath surface. The infrared camera records minor differences of the shroud flowpath surface temperature, Figure 18. Temperature differences are attributed to thermal conductivity variation resulting from defects such as coating cracks, delaminations, or irregularities. Two process improvements which have been incorporated in the procedure are 1) the use of a constant heat source behind the shroud when the infrared picture is taken, and 2) the use of an oscilloscope to maintain a more constant photograph light intensity level.

Three CF6-50 superpeg shrouds were fabricated for NDE inspection and thermal shock testing. Following their fabrication and prior to Lynn thermal shock testing, each shroud was isothermally cycled from 982° C (1800° F) 93° C (200° F) to generate coating flaws. The shrouds were inspected by thermography NDE prior to cycling and at 2, 5, and 10 cycles. The NDE inspection revealed indications of coating flaws in each shroud. During the Lynn thermal shock test the shrouds experienced failure of the braze joint. Post-test examination revealed no evidence of coating delamination or separation. The previous infrared indications were attributed to areas of thin ZrO_2 coating or areas of Hast X superpeg insert delamination (due to poor braze joints).

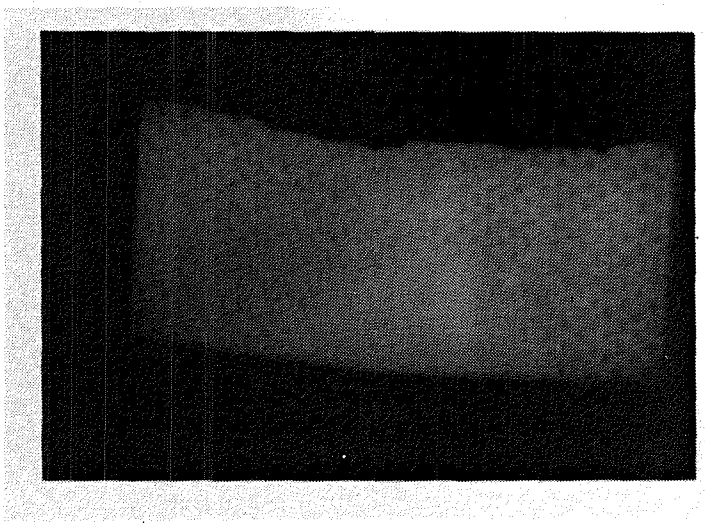

Figure 18. NDE Infra-Red Image of E^3 Ceramic Shroud

Two ZrO_2 coated superpeg shroud castings (no Hast X insert) were also thermal cycled to produce delaminations. The thermal cycle consisted of isothermal exposure at 982° C (1800° F) followed by forced air cooling to room temperature. More severe cycling from 1093° C (2000° F) followed by water quenching was also performed. A total of 40 cycles was accumulated on each shroud. No coating delamination or lifting was visually evident. Periodic infrared inspection did not reveal any coating defects during the intermediate inspection; however, one shroud did contain defect indications after completion of 40 cycles. ZrO_2 coating delamination cracks have been verified in the indicated areas of this particular shroud. Hence, this verified the capability of the infrared technique to discern coating defects.

VI. E^3 ENGINE TEST HARDWARE - PHASE IV

A total of 52 stage 1 high pressure turbine ceramic shrouds were required in two separate lots. Lot 1 contained 28 shrouds, Figure 19, while there were 24 shrouds in Lot 2. The shroud system consisted of the following, René 77 superpeg castings, NiCrAlY bond coat, NiCrAlY/ZrO_2-$8Y_2O_3$ blend coat, and ZrO_2-$8Y_2O_3$ top coat. A metallographic crosssection of this system is shown in Figure 20. Engine test shrouds were sprayed using previously established process parameters with automatic spray equipment and the rotating drum shroud holder. This shroud system had undergone significant development and testing, including thermal shock and CF6-50 engine testing, during the previous phases of this program. All shrouds were inspected using the infrared NDE technique, described in Section V, before and after a one-cycle laboratory thermal shock proof test consisting of a forced air cooled quench of the shroud from 982° C (1800° F).

Two ceramic shrouds from Lot 1 were successfully subjected to 1000 cycles in the Lynn thermal shock test. Post-test infrared NDE inspection revealed no defects and this was confirmed by microscopic examination of one shroud. The thermal shock test was conducted at 1400° C (2500° F) flowpath surface and 793° C (1460° F) backside temperature, followed by forced air cooling to less than 204° C (400° F). Each cycle consisted of three minutes heating to temperature and three minutes cooling. Figures 21 and 22 show the two shrouds after completion of 1000 thermal shock cycles. Discoloration of the coating in the central region was determined, via scanning electron microscopy and EDAX, to be copper contamination from the heating torch. Even under such severe testing conditions no coating spallation occurred, attesting to the excellent thermal shock capability of this ceramic shroud system.

A total of 20 shrouds from Lot 1 have been assembled in the core engine while Lot 2 shrouds are scheduled to complete fabrication in September 1982, and will be held as spares.

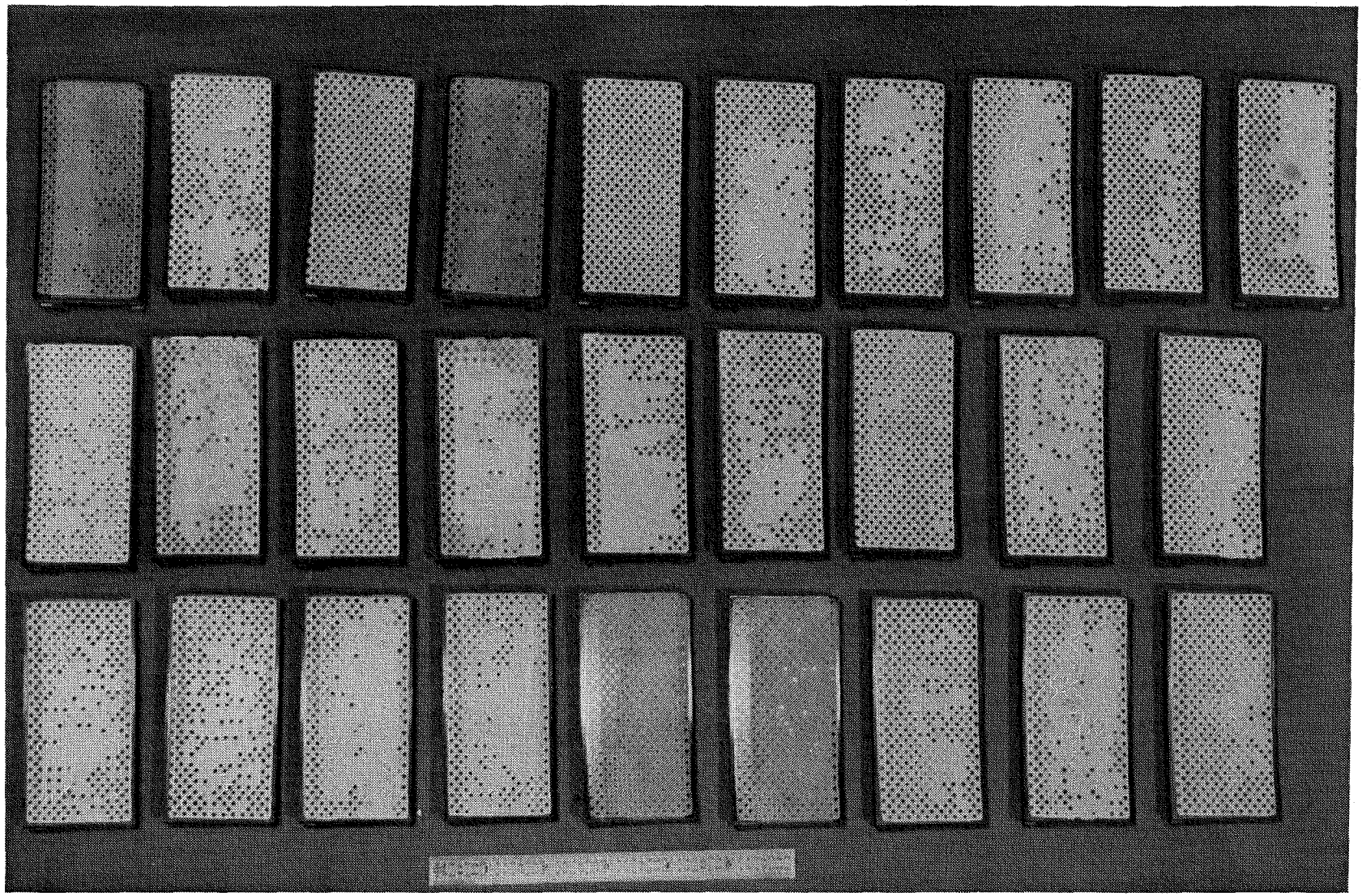

Figure 19. E^3 Fabricated ZrO_2 - $8Y_2O_3$ Ceramic Shrouds

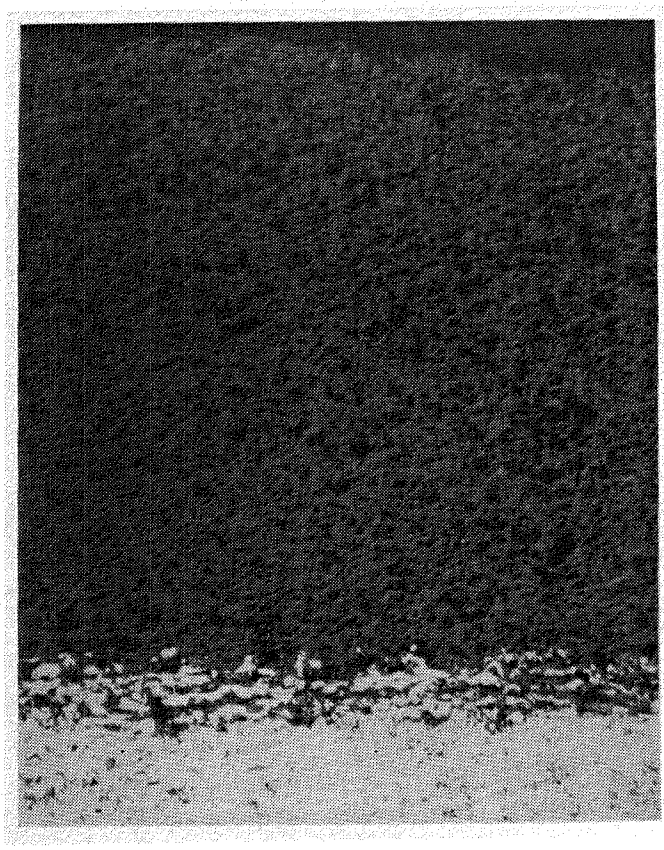

Figure 20. E^3 Ceramic Shroud Coating System

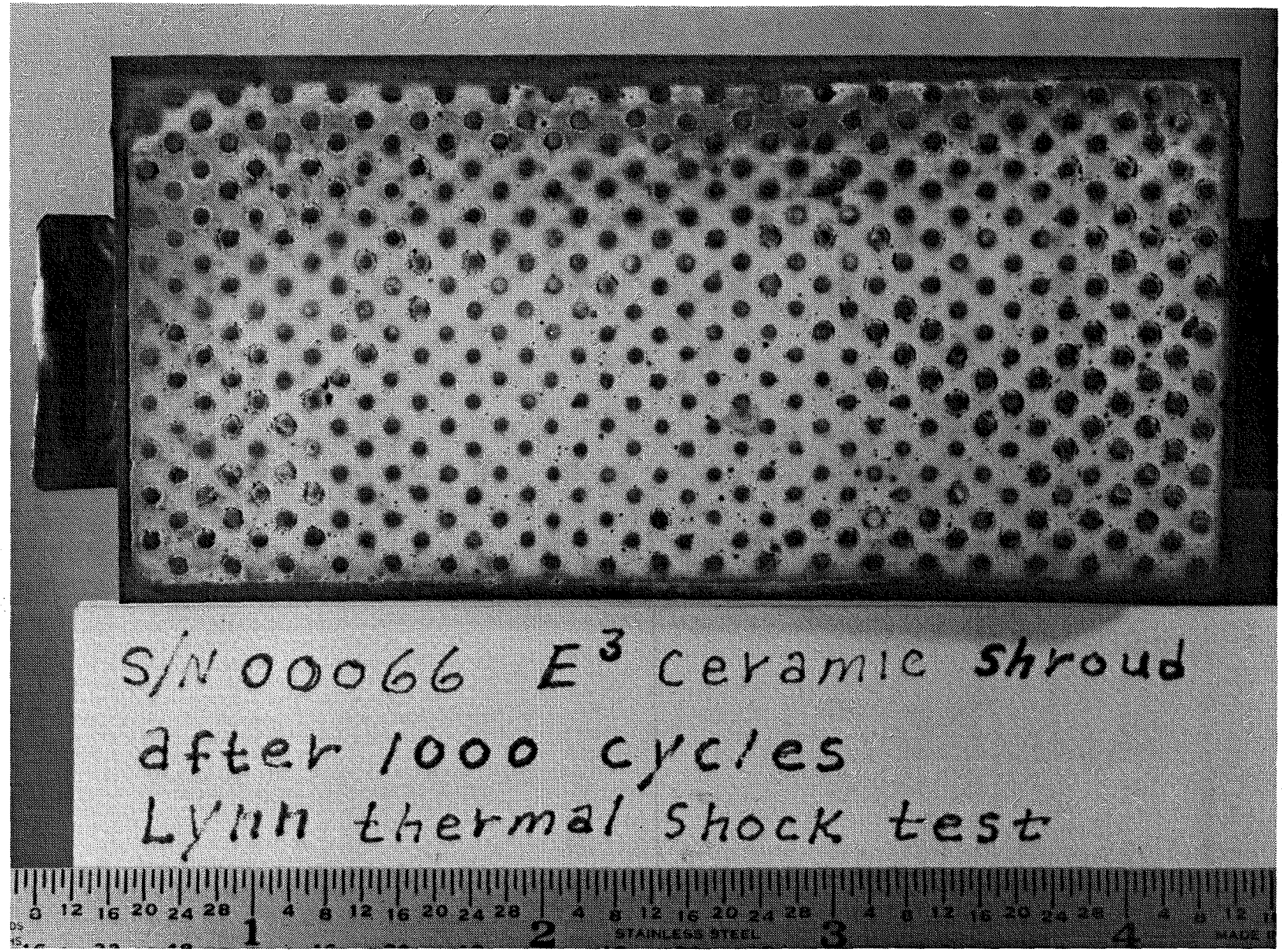

Figure 21. E^3 Ceramic Shroud after 1000 Thermal Shock Cycles

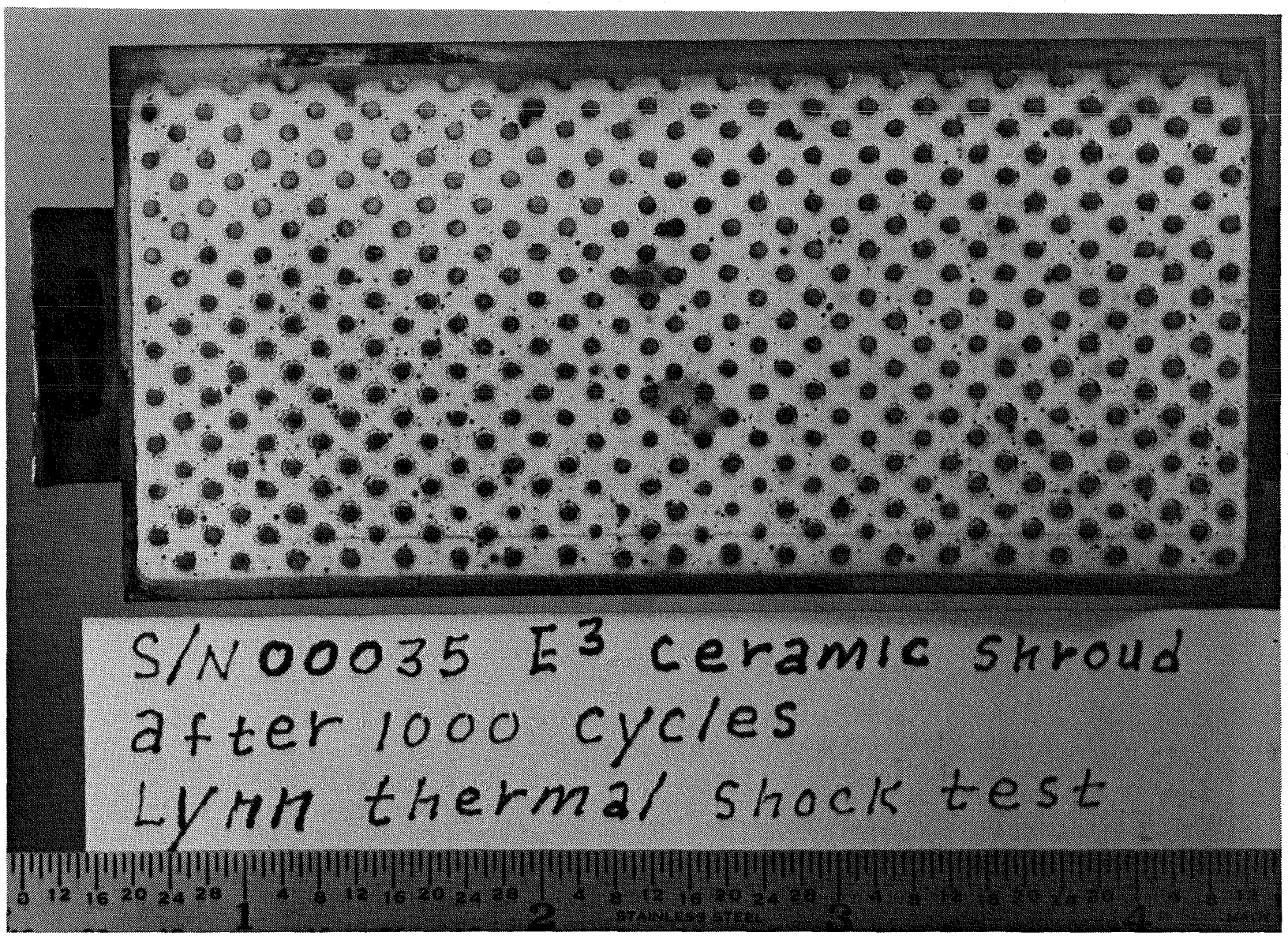

Figure 22. E^3 Ceramic Shroud after 1000 Thermal Shock Cycles

VII. CONCLUSIONS

1. A ceramic shroud system was identified for Energy Efficient Engine Stage 1 High Pressure Turbine. The shroud system consists of the following:

   René superpeg casting

   NiCrAlY bond coating

   NiCrAlY/ZrO_2-$8Y_2O_3$ blend coat

   ZrO_2-$8Y_2O_3$ top coat

2. Fifty-two ceramic (zirconia) shrouds have been fabricated for E^3 engine testing.

3. The superpeg shroud configuration was selected as prime candidate for E^3 engine testing. The wire mesh configuration was backup choice. Standard configuration pegs were found inadequate by the results obtained in the CF6-50 engine tests.

4. Process development and component testing were conducted to establish a process technique for fabricating zirconia shrouds. Automated spraying with a rotating drum shroud holder was determined to produce acceptable shrouds.

5. An infrared non-destructive examination (NDE) technique was developed which shows promising capabilities to inspect zirconia shrouds.

6. Zirconia ceramic shrouds possess adequate engine characteristics as proven by a series of laboratory tests, such as erosion, abradability, hardness, and phase stability, by cyclic thermal shock testing conducted at the Lynn test facility and by three CF6-50 engine tests.

VIII. RECOMMENDATIONS

The following Recommendations are offered:

1. Behavior of zirconia shrouds during engine rub conditions needs to be investigated.

2. Further development should be conducted to improve the reproducibility and interpretation of NDE technique.

3. Continued interaction of design and materials technologists in the development and application of zirconia shrouds is essential for full utilization of ceramic shroud potential in turbine engines.

IX. REFERENCES

1. Bill, R.C.; Wisander, D.C.; and Brewe, D.E. "Preliminary Study of Methods for Providing Thermal Shock Resistance to Plasma-Sprayed Ceramic Gas-Path Seals," AVRADCOM Tech Report 79-28, May 1980.

2. Darolia, R. "Feasibility of SiC Composite Structures for 1644 K (2500° F) Gas Turbine Seal Applications," Final Report NASA contract NAS3-20082, NASA Report NASA CR-159577, November 1979.

3. Bessen, I.I., Rigney, D.V., Schwab, R.C. "Improved High Pressure Turbine Shrouds" Final Report NASA contract NAS3-18905 NASA Report NASA CR-135181 February 1977.

4. Stecura, S. "Effects of Compositional Changes on Performance of a Thermal Barrier Coating System" NASA TM 78-976, August 1978.

APPENDIX A

ENGINE TESTING

ENGINE TESTING

A primary objective of the ceramic shroud engine tests is to determine the effects of the ceramic-to-metal support interface geometry. Variations in ceramic top coat and bond coat were also studied, the objective being to develop an improved shroud design making use of the high temperature capabilities of the ceramic materials. Ceramic offers better oxidation and erosion resistance which can lead to improved engine performance from the reduced amount of cooling air and by maintaining low blade-to-tip clearance. These benefits are achieved by reducing the shroud rub surface material loss and the blade tip wear caused by shroud surface distortion. Since the combination of ceramics and metal is needed to construct this system, an effective and simple means of holding and supporting the ceramic by the metal is required.

Design configurations for selection of ceramics and holding support were studied during the initial phase of the program. The shroud configurations subjected to engine testing had the following features:

1. Wire mesh
2. CF6-50 peg arrangement
3. CF6-50 peg arrangement - submerged pegs
4. Superpeg arrangement

In the CF6-50 peg design arrangement, the ceramic was sprayed, covering the peg to protect it from exposure to the hot gases in one configuration, and also in a configuration whereby the pegs were exposed to the hot gases. Figure A-1 shows a schematic crosssection of the four different bonding techniques used during the development phase.

The first ceramic shrouds were tested in 1979 in the CF6-50 engine. A total running time of 65:22 hours were accumulated in this engine test. Hot gas flowpath temperature was calculated to be up to 1400° C (2550° F) which corrresponds to a ceramic surface temperature of 1271° C (2320° F). Total time at 1370° C (2500° F) to 1400° C (2550° F) turbine rotor inlet temperature was 5:6 hours. Condition of the ceramic shrouds after the tests is

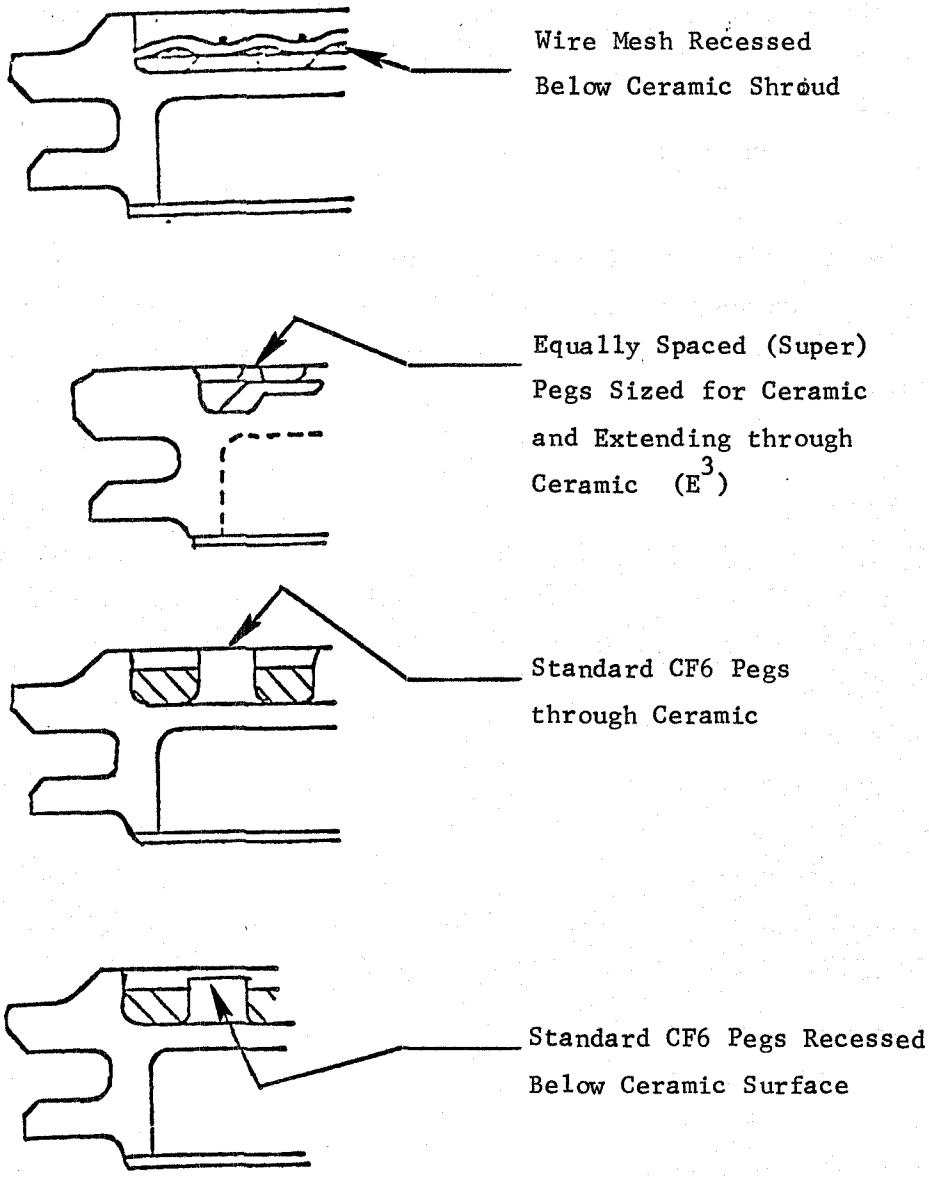

Figure A-1 Engine Test Ceramic Shrouds Characteristics

shown in Figures A-2 and A-3. Condition and evaluation of the shrouds after testing showed the wire mesh configuration to contain considerable more surface cracks than the superpeg. The E^3 design superpeg shrouds shown in Figure A-2 were observed to be in very good condition. The shrouds with the CF6-50 peg design had experienced various degrees of spallation as shown in Figure A-3.

From this first meaningful test, the conclusion was reached to continue testing the shrouds containing the wire mesh and superpeg configuration. Also as a result of this test, sufficient confidence was gained to continue with the integral ceramic-metal shroud concept in an engine system performing cyclic type tests.

For the second CF6-50 engine tests, the plan was to run the ceramic shrouds for 1500 "C" cycles. The duration and flight conditions simulating a "C" cycle are shown in Figure A-4. The two shroud designs, the superpeg, and the wire mesh were engine tested: a total of ten shrouds were installed in this engine. The total running time completed was 166:46 hours, and 625 "C" cycles were completed before the test was prematurely terminated by unrelated damage sustained in the engine. Occurrences at the time of the test termination involved overtemperature by some 110° C (200° F) with some impact damage sustained to the shrouds. Total time above 1370° C (2500° F) gas stream temperature was 21 hours. Shroud temperatures were in the order of 1304° C (2380° F) to 1250° C (2280° F).

Inspection of the ceramic shrouds after the tests showed the superpeg design to be in excellent condition. The wire mesh ceramic shroud exhibited evidence of erosion of the ceramic layer. Although turbine overtemperature had occurred, the test provided further results of the durability and operating experience gained for the E^3 ceramic shroud design with the superpeg.

The third test consisted of a planned engine running for 750 "C" cycles. Four of the shrouds were of the superpeg design and four were of the wire mesh design. Completion of the engine tests for 750 "C" cycles and 208:27 hours at turbine rated temperatures showed the superpeg design parts to be in good condition and much superior to the wire mesh parts.

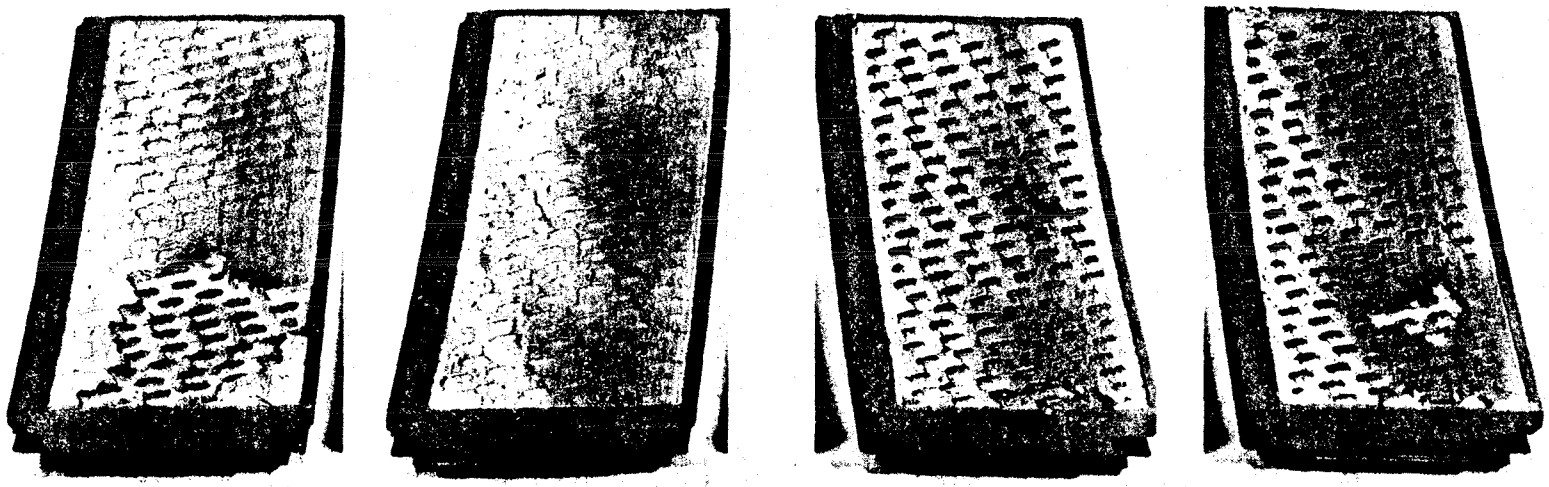

20 mil (Half Height) Peg Array **40 mil (Full Height) Peg Array**

455-105/10
65:22 hours

Figure A-2. Zirconia Oxide Shrouds, CF6-50 Engine - 1979 Test

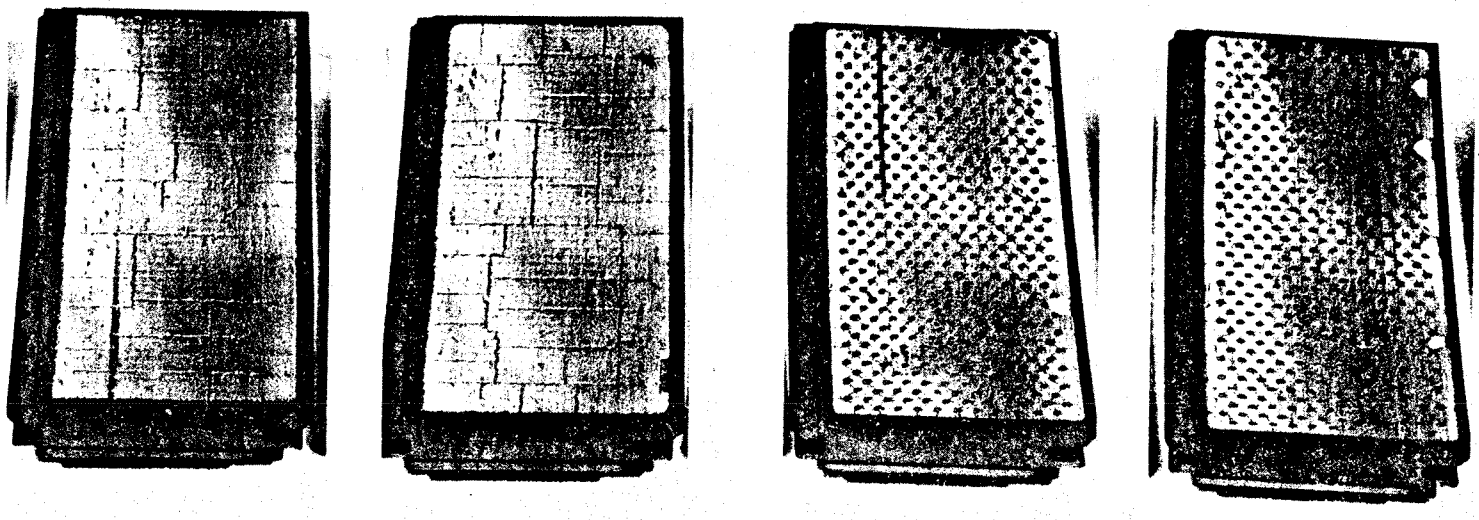

Wire Mesh

E^3 Manufacturing Shrouds

455-105/10
65:22 hours

Figure A-3. Zirconia Oxide Shrouds (With Standard Cf6 Pegs, CF6-50 Engine Test - 1979 Test

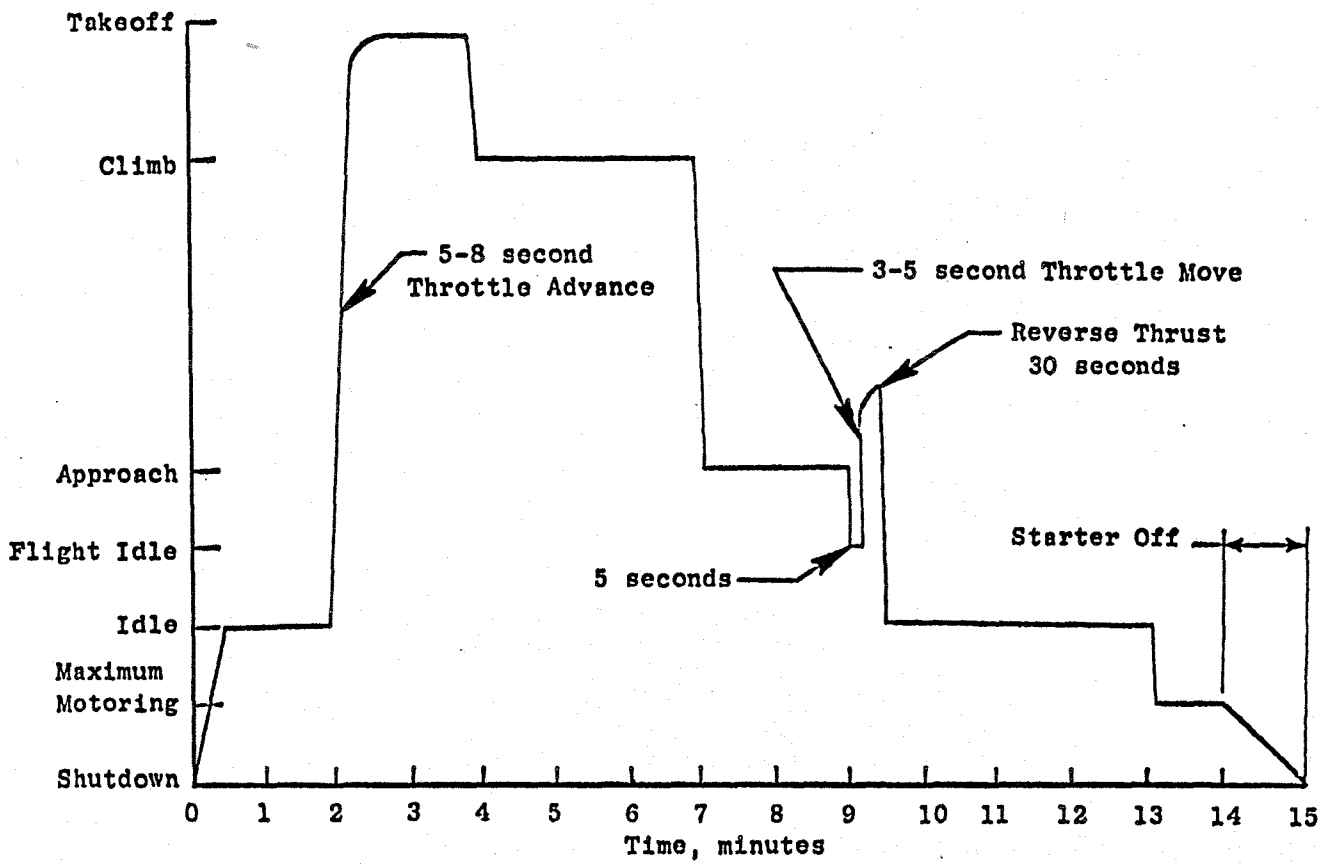

Figure A-4. CF6-50 Engine Endurance Test "C" Cycle

Visual examination showed that the four superpeg shrouds had no spalling and are in good condition for continued engine testing. The wire mesh ceramic shrouds had significant loss of the ceramic face material, some in the top coat and some down into the mesh. Further testing is planned in a CF6-50 engine for 1000 "C" cycles using two of the superpeg shrouds which were tested for 750 "C" cycles.

The E^3 superpeg design type ceramic shrouds have accumulated to date a total of 1375 "C" cycles. These shrouds have shown the reliability and soundness of the design based on the engine tests.

The E^3 core and ICLS engine tests contain a full set (except four shrouds used for the clearance measurement) of the superpeg design. Commitment to the E^3 design was made possible by the extensive CF6-50 engine tests run at power conditions and time which simulates actual aircraft use.

The summary of the ceramic testing accomplished is recorded in Table A-1.

Table A-1. Summary of Ceramic Shroud CF6-50 Engine Testing.

YEAR	ENGINE	HOURS	CYCLES	CERAMIC SHROUD TYPE	PERFORMANCE
1979	CF6-50 455-105/10	65:22	SMP - not cycled	Peg/ wire mesh	Minor spalling - led to changes in configuration and material.
1980	CF6-50 455-508-20	166:45	625 "C"	Peg/ wire mesh	Shrouds bent after blade failure. Ceramic intact.
1981	CF6-50 455-509/9A	208:27	750 "C"	Peg/ wire mesh	Good condition for continued running (Peg configuration).
TOTAL HOURS		440:56			

DISTRIBUTION

NASA Headquarters
600 Independence Avenue, SW
Washington, DC 20546
Attention: RTP-6/R.S. Colladay
RTP-6/C.C. Rosen
RTP-6/J. Facey
RTM-6/L. Harris

NASA-Lewis Research Center
21000 Brookpark Road
Cleveland, OH 44135

Attention:	D.L. Nored	MS 301-2
	C.C. Ciepluch	MS 301-4 (18 copies)
	J.W. Schaefer	MS 301-4
	P.G. Batterton	MS 301-4
	G.K. Sievers	MS 301-2
	M.A. Beheim	MS 3-5
	M.J. Hartmann	MS 3-7
	R.A. Rudey	MS 86-5
	W.C. Strack	MS 501-10
	T.P. Moffitt	MS 77-2
	R.E. Jones	MS 86-6
	L.J. Kiraly	MS 23-2
	D.C. Mikkelson	MS 86-1
	A. Long	MS 500-305
	J.F. Groeneweg	MS 54-3
	W.M. Braithwaite	MS 500-208
	J.C. Williams	MS 500-211
	R.L. Davies	MS 106-1
	R.H. Johns	MS 49-6
	L.J. Kaszubinski	MS 86-2
	J.F. Sellers	MS 100-1
	J.R. Mihaloew	MS 100-1
	L. Reid	MS 5-9
	D.W. Drier	MS 86-2
	R.W. Niedzwiecki	MS 86-6
	AFSC Liaison Office	MS 501-3
	ARMY R&T Propulsion Lab	MS 302-2

NASA Ames Research Center
Moffett Field, CA 94035
Attention: 202-7/M.H. Waters

NASA Langley Research Center
Langley Field, VA 23365
Attention: R. Leonard
D. Maiden
L.J. Williams

NASA Dryden Flight Research Center
P.O. Box 273
Edwards, CA 93523
Attention: J.A. Albers

Department of Defense
Washington, DC 20301
Attention: R. Standahar 3D1089 Pentagon

Wright-Patterson Air Force Base
Dayton, OH 45433
Attention: APL Chief Scientist
E.E. Abell
H.I. Bush
E.E. Bailey (NASA Liaison)
R.P. Carmichael
R. Ellis
W.H. Austin, Jr.

AFWAL/PS
ASD/YZE
AFWAL/POT
AFWAL/NASA
ASD/XRHI
ASD/YZN
ASD/ENF

Eustis Directorate
U.S. Army Air Mobility
R&D Laboratory
Fort Eustis, VA 23604
Attention: J. Lane, SAVDL-EU-Tapp

Department of Transportation
NASA/DOT Joint Office of
Noise Abatement
Washington, D.C. 20590
Attention: C. Foster

NAVY Department
Naval Air Systems Command
Washington, DC 20361
Attention: W. Koven AIR-03E
J.L. Byers AIR-53602
E.A. Lichtman AIR-330E
G. Derderian AIR-5362C

Federal Aviation Administration
Noise Abatement Division
Washington, DC 20590
Attention: E. Sellman AEE-120

NAVAL Air Propulsion Test Center
Trenton, NJ 08628
Attention: J.J. Curry
A.A. Martino

Rohr Corporation
P.O. Box 1516
Chuyla Vista, CA 92012
Attention: James C. Fuscoe

U.S. Naval Air Test Center
Code SY-53
Patuxent River, MD 20670
Attention: E.A. Lynch

TRW Equipment
TRW Inc.
23555 Euclid Ave.
Cleveland, Ohio 44117
Attention: I. Toth

USAVRAD Command
P.O. Box 209
St. Louis, MO 63166
Attention: Robert M. Titus

Federal Aviation Administration
12 New England Executive Park
Burlington, MA 18083
Attention: Jack A. Sain, ANE-200

Detroit Diesel Allison Div. G.M.C.
333 West First St.
Dayton, OH 45202
Attention: F.H. Walters

Curtiss Wright Corporation
Woodridge, NJ 07075
Attention: S. Lombardo
S. Moskowitz

AVCO/Lycoming
550 S. Main Street
Stratford, CN 06497
Attention: H. Moellmann

Williams Research Co.
2280 W. Maple Road
Walled Lake, MI 48088
Attention: R. VanNimwegen
R. Horn

Teledyne CAE, Turbine Engines
1330 Laskey Road
Toledo, OH 43612
Attention: R.H. Gaylord

Pratt & Whitney Aircraft Group/UTC
Government Products Division
P.O. Box 2691
West Palm Beach, FL 33402
Attention: B.A. Jones

Boeing Commercial Airplane Co.
P.O. Box 3707
Seattle, WA 98124
Attention: P.E. Johnson MS 9H-46
D.C. Nordstrom MS-73-01

Brunswick Corporation
2000 Brunswick Lane
Deland, FL 32720
Attention: A. Erickson

Delta Airlines, Inc.
Hartsfield-Atlanta International Airport
Atlanta, GA 30320
Attention: C.C. Davis

FluiDyne Engineering Corp.
5900 Olson Memorial Highway
Minneapolis, MN 55422
Attention: J.S. Holdhusen

Massachusetts Inst. of Technology
Dept. of Astronautics & Aeronautics
Cambridge, MA 02139
Attention: Mames Mar

Detroit Diesel Allison Div. G.M.C.
P.O. Box 894
Indianapolis, IN 46202
Attention: W.L. McIntire

The Garrett Corporation
AIResearch Manufacturing Co.
Torrance, CA 90509
Attention: F.E. Faulkner

The Garrett Corporation
AIResearch Manufacturing Co.
402 S. 36 Street
Phoenix, AZ 85034
Attention: Library

General Electric Co./AEG
1000 Western Avenue
Lynn, MA 01910
Attention: R.E. Nietzel

Pratt & Whitney Aircraft Group/UTC
Commercial Products Division
East Hartford, CT 06108
Attention: W. Gardner (3 copies)
I. Mendelson

Douglas Aircraft Co.
McDonnell Douglas Corp.
3855 Lakewood Boulevard
Long Beach, CA 90846
Attention: R.T. Kawai Code 36-41
M. Klotzsche 36-41

AIResearch Manufacturing Co.
111 South 34th Street
P.O. Box 5217
Phoenix, AZ 85010
Attention: C.E. Corrigan
(930120/503-4F)

American Airlines
Maint. & Engrg. Center
Tulsa, OK 74151
Attention: W.R. Neeley

Lockheed California Co.
Burbank, CA 91502
Attention: J.F. Stroud, Dept. 75-42
R. Tullis, Dept. 74-21

Grumman Aerospace Corp.
South Oyster Bay Road
Bethpage, NY 11714
Attention: C. Hoeltzer

End of Document